Eur. Phys. J. C (2022) 82:229
https://doi.org/10.1140/epjc/s10052-022-10148-9

THE EUROPEAN PHYSICAL JOURNAL C

Regular Article - Theoretical Physics

Two-loop prediction of the anomalous magnetic moment of the muon in the Two-Higgs Doublet Model with GM2Calc 2

Peter Athron[1,2], **Csaba Balazs**[2], **Adriano Cherchiglia**[3], **Douglas Jacob**[2,a], **Dominik Stöckinger**[4], **Hyejung Stöckinger-Kim**[4], **Alexander Voigt**[5]

[1] Department of Physics and Institute of Theoretical Physics, Nanjing Normal University, Nanjing 210023, Jiangsu, China
[2] ARC Centre of Excellence for Particle Physics at the Terascale, School of Physics, Monash University, Melbourne, VIC 3800, Australia
[3] Centro de Ciêcias Naturais e Humanas, Universidade Federal do ABC, Santo André, Brazil
[4] Institut für Kern- und Teilchenphysik, TU Dresden, Zellescher Weg 19, 01069 Dresden, Germany
[5] Fachbereich Energie und Biotechnologie, Hochschule Flensburg, Kanzleistraße 91–93, 24943 Flensburg, Germany

Received: 24 November 2021 / Accepted: 21 February 2022

Abstract We present an extension of the GM2Calc software to calculate the muon anomalous magnetic moment (a_μ^{BSM}) in the Two-Higgs Doublet Model. The Two-Higgs Doublet Model is one of the simplest and most popular extensions of the Standard Model. It is one of the few single field extensions that can give large contributions to a_μ^{BSM}. It is essential to include two-loop corrections to explain the long standing discrepancy between the Standard Model prediction and the experimental measurement in the Two-Higgs Doublet Model. The new version GM2Calc 2 implements the state of the art two-loop calculation for the general, flavour violating Two-Higgs Doublet Model as well as for the flavour aligned Two-Higgs Doublet Model and the type I, II, X and Y flavour conserving variants. Input parameters can be provided in either the gauge basis or the mass basis, and we provide an easy to use SLHA-like command-line interface to specify these. Using this interface users may also select between Two-Higgs Doublet Model types and choose which contributions to apply. In addition, GM2Calc 2 also provides interfaces in C++, C, Python and Mathematica, to make it easy to interface with other codes.

Contents

1 Introduction

The anomalous magnetic moment of the muon, a_μ, is one of the most important observables in particle physics. Its importance stems from the fact that it is one of the most precisely measured physical quantities and that it is very sensitive to new physics as well as the strong, weak and electromagnetic interactions of the Standard Model (SM). The significance of a_μ has increased further in the wake of the recent release of the first results from the Fermilab Muon $g-2$ experiment [1]. This collaboration found, in combination with the results from the Brookhaven National Laboratory [2], an experimental value of

[a] e-mail: douglas.jacob@monash.edu (corresponding author)

Published online: 15 March 2022

$$a_\mu^{\text{Exp}} = (11659206.1 \pm 4.1) \times 10^{-10}. \tag{1}$$

The SM prediction from the Muon $g-2$ Theory Initiative White Paper [3] is

$$a_\mu^{\text{SM}} = (11659181.0 \pm 4.3) \times 10^{-10}, \tag{2}$$

which combines quantum electrodynamic contributions [4,5], electroweak contributions [6,7], hadronic vacuum-polarization [8–14] and light-by-light contributions [15–29].[1] The experimental measurement differs from the SM prediction by 4.2σ which suggests a beyond the Standard Model (BSM) contribution of

$$a_\mu^{\text{BSM}} = (25.1 \pm 5.9) \times 10^{-10}. \tag{3}$$

The high precision in both the experimental measurement and the SM theoretical prediction requires BSM contributions to be known with a similar level of accuracy.

The Two-Higgs Doublet Model (2HDM) is one of the simplest and most widely studied extensions of the SM (see e.g. Ref. [42] for a review or the relevant chapters of Ref. [43]). Although the 2HDM has been studied for many decades and the only Higgs boson discovered is closely SM-like [44,45], interest in this model has not waned, and recent progress has been achieved e.g. on LHC interpretations [46–50], B-physics [51–55], theoretical constraints [56–60], electroweak phase transitions in the early universe [61–65], precision calculations of Higgs decays [66–74]. Remarkably, the 2HDM is one of the very few single field extensions of the Standard Model that can explain the deviation between a_μ^{Exp} and a_μ^{SM} [75] while satisfying existing constraints from collider physics searches and other observables.

A second Higgs doublet that can couple to SM fermions generically induces large tree-level flavour changing neutral currents at odds with experiment. Due to this 2HDM s are often classified according to the discrete symmetries imposed to conserve flavour, giving four types [76]: type I [77], type II [78], type X (often called the lepton specific 2HDM) [79,80] and type Y (sometimes refereed to as the flipped 2HDM) [81,82]. Large flavour changing neutral currents can also be avoided by assuming an alignment in flavour space between the Yukawa matrices of the two doublets, giving the so-called flavour-aligned 2HDM (FA2HDM) [83,84]. After the first results of the LHC, Ref. [85] systematically investigated the phenomenology of all 2HDM versions with discrete symmetries and showed that among them, only the type X variant is able to provide significant contributions to a_μ. The type X explanation of the deviation between a_μ^{Exp} and a_μ^{SM} has been further explored in Refs. [86–99]. The more general flavour-aligned 2HDM and its contributions to a_μ were studied in Refs. [75,100–104]. Other variants, including more general realisations that allow for Higgs-mediated flavour violation were investigated in Refs. [105–112].

Phenomenological investigations of BSM physics are greatly enhanced by the use of precise software tools. These tools can automate the calculation of precision corrections, or provide numerical methods to quickly and reliably solve related problems. For example in the 2HDM one is often concerned that a particular benchmark point respects measured limits of electroweak oblique parameters, or that the new couplings and bosons do not provide contributions to Higgs decays which violate collider constraints. For the 2HDM a widely used software package is `2HDMC` [113], which provides calculations of the spectrum, decays, oblique S, T and U parameters as well as a calculation of the 2HDM new physics contributions to a_μ. There also exists the tool `ScannerS` [114] which can place theoretical, experimental, dark matter, and electroweak phase transition constraints on extended scalar sectors, including the 2HDM. A more precise calculation of the decays is available from the 2HDM decay dedicated code `2HDECAY` [115], while `PROPHECY4F` [116] provides a package which focuses on calculating $h \to WW/ZZ \to 4f$ decays. Additionally, the tools `HiggsBounds` [117–121] and `HIGGSSIGNALS` [122–124] allow one to place constraints on the Higgs sectors of BSM physics through the measured behaviour of Higgs bosons from collider search experiments.

Higher precision calculations for the spectrum, decays and other observables in the 2HDM are also available for arbitrary user-defined extensions of the SM through codes such as `SARAH/SPheno` [125–130] and `FlexibleSUSY` [131–134] (with decays recently added in `FlexibleDecay` [134]) where model files for the 2HDM are already distributed. Additionally, both packages provide one-loop contributions to a_μ^{BSM}. For two-loop contributions to a_μ^{BSM} in the MSSM, `FlexibleSUSY` links to the dedicated tool `GM2Calc` [135]. For the 2HDM there was no such option until now. Here we extend `GM2Calc` with the 2HDM to provide a program which includes state of the art two-loop level contributions of Ref. [102] to the anomalous magnetic moment of the muon.

The 2HDM contributions implemented in `GM2Calc` version 2 include the one-loop contributions, the two-loop fermionic corrections (including the well-known Barr-Zee diagrams), and the complete set of bosonic two-loop correc-

[1] As discussed extensively in the Theory Initiative White Paper [3], the proposed SM prediction does not use lattice gauge theory evaluations of the hadronic vacuum polarization. The lattice world average evaluated in Ref. [3], based on [30–38], is compatible with the data-based result [8–14], has a higher central value and larger uncertainty. However more recent lattice results are obtained in Refs. [39,40], and in particular Ref. [39] obtains a result with smaller uncertainty, which would shift the SM prediction for a_μ closer to the experimental value. Scrutiny of these results is ongoing (see e.g. Ref. [41]) and further progress can be expected.

tions. The one-loop contributions are of the order $\mathcal{O}(m_\mu^4)$ and therefore usually subdominant. The two-loop contributions arise at $\mathcal{O}(m_\mu^2)$ and are implemented at this order. Ref. [102] has assumed the flavour-aligned 2HDM with vanishing couplings $\lambda_{6,7}$, but here we relax this assumption and allow the more general case. The 2HDM version of `GM2Calc 2` allows the user to input deviations from the aligned limit, as well as select any one of the 2HDM types I, II, X or Y. Just like version 1, `GM2Calc 2` allows the user to input parameter information using an SLHA-like [136,137] input file. We also provide interfaces in C, C++, `Python` and `Mathematica` to make it easy to link to other public codes. Furthermore, `GM2Calc 2` (hereafter `GM2Calc`) can be used as a standalone tool for studies of a_μ in the 2HDM, or to explore the 2HDM phenomenology more broadly it can be used in combination with other codes via the SLHA interface. For example, `GM2Calc` can be called alongside `FlexibleSUSY`, or in combination with other standalone tools like `2HDECAY` or alongside the `2HDMC` package, replacing its native calculation of the anomalous magnetic moment of the muon. The MSSM calculation is already available in `GAMBIT` [138,139] and it should be straightforward to extend this to also use the 2HDM calculation in future versions.

The rest of this paper is divided into the following sections. Section 2 provides a pedagogical introduction to the 2HDM, giving the Lagrangian both before and after electroweak symmetry breaking, and defining the Yukawa couplings in the various types of the 2HDM. There we give the one- and two-loop contributions to a_μ^{BSM}, and the uncertainty estimate for the calculation. Section 3 describes various ways to use the 2HDM in `GM2Calc`. It also shows how to interface `GM2Calc` using C++, C, `Python` and `Mathematica`. Finally, Sect. 4 demonstrates various possible ways `GM2Calc` can be applied to calculate the BSM contributions to the anomalous magnetic moment of the muon in the 2HDM.

2 Review of 2HDM and implemented contributions to a_μ

2.1 The Model

The Two-Higgs Doublet Model (2HDM) extends the Standard Model (SM) with an additional scalar SU(2) doublet. We denote the two complex Higgs SU(2) doublets in the 2HDM as Φ_i $(i = 1, 2)$,

$$\Phi_i = \begin{pmatrix} a_i^+ \\ \frac{1}{\sqrt{2}}(v_i + b_i + \mathrm{i}c_i) \end{pmatrix}, \tag{4}$$

where b_i and c_i are real scalar fields and a_i^+ are complex scalar fields. Each Higgs doublet acquires a real non-zero vacuum expectation value (VEV), v_i, which satisfy

$$\tan\beta = \frac{v_2}{v_1}, \quad v^2 = v_1^2 + v_2^2, \tag{5}$$

with $0 \leq \beta \leq \pi/2$ and $v \approx 246\,\text{GeV}$, which implies $v_1 = v\cos\beta$ and $v_2 = v\sin\beta$. The extended Lagrangian includes the Higgs potential $\mathcal{L}_{\text{Scalar}}$ and the Yukawa interaction part $\mathcal{L}_{\text{Yuk}}$,

$$\mathcal{L} \ni \mathcal{L}_{\text{Scalar}} + \mathcal{L}_{\text{Yuk}}. \tag{6}$$

The most general form of Higgs potential is

$$\begin{aligned} -\mathcal{L}_{\text{Scalar}} = {} & m_{11}^2\Phi_1^\dagger\Phi_1 + m_{22}^2\Phi_2^\dagger\Phi_2 - \left[m_{12}^2\Phi_1^\dagger\Phi_2 + \text{h. c.}\right] \\ & + \frac{1}{2}\lambda_1\left(\Phi_1^\dagger\Phi_1\right)^2 + \frac{1}{2}\lambda_2\left(\Phi_2^\dagger\Phi_2\right)^2 \\ & + \lambda_3\left(\Phi_1^\dagger\Phi_1\right)\left(\Phi_2^\dagger\Phi_2\right) + \lambda_4\left(\Phi_1^\dagger\Phi_2\right)\left(\Phi_2^\dagger\Phi_1\right) \\ & + \left[\frac{1}{2}\lambda_5\left(\Phi_1^\dagger\Phi_2\right)^2 + \lambda_6\left(\Phi_1^\dagger\Phi_1\right)\left(\Phi_1^\dagger\Phi_2\right)\right. \\ & \left. + \lambda_7\left(\Phi_2^\dagger\Phi_2\right)\left(\Phi_1^\dagger\Phi_2\right) + \text{h. c.}\right], \end{aligned} \tag{7}$$

where λ_5, λ_6, λ_7 and m_{12}^2 are real for the CP-conserving Higgs potential. The mass eigenstates of Higgs and Goldstone bosons h, H, A, H^+, G^0 and G^+ are obtained as

$$\begin{pmatrix} h \\ H \end{pmatrix} = Z_{\mathcal{H}^0}\mathcal{H}^0, \quad \begin{pmatrix} G^0 \\ A \end{pmatrix} = Z_{\mathcal{A}}\mathcal{A}, \quad \begin{pmatrix} G^+ \\ H^+ \end{pmatrix} = Z_{\mathcal{H}^+}\mathcal{H}^+, \tag{8}$$

with

$$\mathcal{H}^0 = \begin{pmatrix} b_1 \\ b_2 \end{pmatrix}, \qquad \mathcal{A} = \begin{pmatrix} c_1 \\ c_2 \end{pmatrix}, \qquad \mathcal{H}^+ = \begin{pmatrix} a_1^+ \\ a_2^+ \end{pmatrix}, \tag{9}$$

from Eq. (7). The orthogonal matrices $Z_{\mathcal{H}^0}$, $Z_{\mathcal{A}}$ and $Z_{\mathcal{H}^\pm}$ for Eq. (8) are given as

$$\begin{aligned} & Z_{\mathcal{H}^0} = \begin{pmatrix} -\sin\alpha & \cos\alpha \\ \cos\alpha & \sin\alpha \end{pmatrix}, \qquad Z_{\mathcal{A}} = \begin{pmatrix} \cos\beta & \sin\beta \\ -\sin\beta & \cos\beta \end{pmatrix}, \\ & Z_{\mathcal{H}^+} = \begin{pmatrix} \cos\beta & \sin\beta \\ -\sin\beta & \cos\beta \end{pmatrix}. \end{aligned} \tag{10}$$

The corresponding mass square matrices $M_{\mathcal{H}^0}^2$, $M_{\mathcal{A}}^2$ and $M_{\mathcal{H}^+}^2$ for $\mathcal{H}^0$, $\mathcal{A}$ and $\mathcal{H}^+$ in Eq. (9), respectively, are diagonalized as

$$\begin{aligned} & M_{\mathcal{H}^0}^2 = Z_{\mathcal{H}^0}^\dagger(M_{\mathcal{H}^0}^D)^2 Z_{\mathcal{H}^0}, \qquad M_{\mathcal{A}}^2 = Z_{\mathcal{A}}^\dagger(M_{\mathcal{A}}^D)^2 Z_{\mathcal{A}}, \\ & M_{\mathcal{H}^+}^2 = Z_{\mathcal{H}^+}^\dagger(M_{\mathcal{H}^+}^D)^2 Z_{\mathcal{H}^+}. \end{aligned} \tag{11}$$

The Higgs boson mass eigenvalues are denoted as

$$M^D_{\mathcal{H}^0} = \mathrm{diag}(m_h, m_H),\ M^D_{\mathcal{A}} = \mathrm{diag}(m_{G^0}, m_A),$$
$$M^D_{\mathcal{H}^\pm} = \mathrm{diag}(m_{G^\pm}, m_{H^\pm}), \tag{12}$$

where in Feynman gauge $m_{G^+} = m_W$ and $m_{G^0} = m_Z$. We chose the CP-even Higgs boson mixing angle α such that $-\pi/2 \le \beta - \alpha \le \pi/2$ [113].

The general form of the Yukawa interaction Lagrangian is given as

$$-\mathcal{L}_{\text{Yuk}} = \Gamma^0_d \overline{q^0_L} \Phi_1 d^0_R + \Gamma^0_u \overline{q^0_L} \Phi^c_1 u^0_R + \Gamma^0_l \overline{l^0_L} \Phi_1 e^0_R + \Pi^0_d \overline{q^0_L} \Phi_2 d^0_R + \Pi^0_u \overline{q^0_L} \Phi^c_2 u^0_R + \Pi^0_l \overline{l^0_L} \Phi_2 e^0_R + \text{h. c.} \tag{13}$$

where $\Phi^c_i \equiv \mathrm{i}\sigma^2 \Phi^*_i$, and q^0_L, l^0_L, u^0_R, d^0_R, and e^0_R are fermion gauge eigenstates.[2] In general the Yukawa coupling matrices, Γ^0_f and Π^0_f $(f = u, d, l)$ are complex and non-diagonal 3×3 matrices which can not be simultaneously diagonalized, which produces flavour changing neutral currents (FCNC).

From the Yukawa interaction Lagrangian in Eq. (13) the 3×3 fermion mass matrices M_f $(f = u, d, l)$ are obtained as

$$M_u = \frac{1}{\sqrt{2}} \left(v_1 \Gamma^0_u + v_2 \Pi^0_u \right), \tag{14}$$
$$M_d = \frac{1}{\sqrt{2}} \left(v_1 \Gamma^0_d + v_2 \Pi^0_d \right), \tag{15}$$
$$M_l = \frac{1}{\sqrt{2}} \left(v_1 \Gamma^0_l + v_2 \Pi^0_l \right). \tag{16}$$

The fermion mass matrices are diagonalized using singular value decomposition. The diagonal fermion mass matrices M^D_f $(f = u, d, l)$ are given by

$$M_u = V^\dagger_u M^D_u U_u, \quad \text{with} \quad M^D_u = \mathrm{diag}(m_u, m_c, m_t), \tag{17}$$
$$M_d = V^\dagger_d M^D_d U_d, \quad \text{with} \quad M^D_d = \mathrm{diag}(m_d, m_s, m_b), \tag{18}$$
$$M_l = V^\dagger_l M^D_l U_l, \quad \text{with} \quad M^D_l = \mathrm{diag}(m_e, m_\mu, m_\tau), \tag{19}$$

where V_f and U_f are unitary matrices, and the corresponding fermion mass eigenstates $f = u, d, l$ are obtained as

$$f_L = V_f f^0_L, \quad \text{and} \quad f_R = U_f f^0_R. \tag{20}$$

By combining Eq. (5) and Eqs. (14)–(16), Γ^0_u, Γ^0_d and Γ^0_l can be expressed in terms of M_f and Π^0_f as

$$\Gamma^0_f = \frac{\sqrt{2} M_f}{v \cos\beta} - \Pi^0_f \tan\beta. \tag{21}$$

[2] The Γ^0 and Π^0 matrices correspond to η_1 and η_2 in Ref. [42], see their Eq. (92).

The Yukawa interaction Lagrangian Eq. (13) can be also written in the so-called Higgs basis, where only one Higgs doublet has non-zero VEV. This can be obtained by rotating $\Phi_{1,2}$ and the Yukawa matrices as

$$\begin{pmatrix} \Phi_v \\ \Phi_\perp \end{pmatrix} = \begin{pmatrix} \cos\beta & \sin\beta \\ -\sin\beta & \cos\beta \end{pmatrix} \begin{pmatrix} \Phi_1 \\ \Phi_2 \end{pmatrix}, \tag{22}$$
$$\begin{pmatrix} \Sigma^0_f \\ \rho^0_f \end{pmatrix} = \begin{pmatrix} \cos\beta & \sin\beta \\ -\sin\beta & \cos\beta \end{pmatrix} \begin{pmatrix} \Gamma^0_f \\ \Pi^0_f \end{pmatrix}, \tag{23}$$

such that only Φ_v has the VEV v and Σ^0_f are its Yukawa couplings. It contains the SM-like Goldstone bosons, whereas the second field $\Phi_\perp$ contains non-SM Higgs bosons $H^\pm$ and A, and its Yukawa couplings ρ^0_f are important parameters in the 2HDM.[3] With this transformation the Yukawa interaction Lagrangian becomes

$$-\mathcal{L}_{\text{Yuk}} = \Sigma^0_d \overline{q^0_L} \Phi_v d^0_R + \Sigma^0_u \overline{q^0_L} \Phi^c_v u^0_R + \Sigma^0_l \overline{l^0_L} \Phi_v e^0_R + \rho^0_d \overline{q^0_L} \Phi_\perp d^0_R + \rho^0_u \overline{q^0_L} \Phi^c_\perp u^0_R + \rho^0_l \overline{l^0_L} \Phi_\perp e^0_R + \text{h. c.} \tag{24}$$

In this way, the fermion masses are purely generated from the Higgs doublet Φ_v, and the fermion mass matrices in Eqs. (14)–(16) become

$$M_u = \frac{v}{\sqrt{2}} \Sigma^0_u, \quad M_d = \frac{v}{\sqrt{2}} \Sigma^0_d, \quad M_l = \frac{v}{\sqrt{2}} \Sigma^0_l, \tag{25}$$

which implies $V_f \Sigma^0_f U^\dagger_f = \sqrt{2} M^D_f / v$. In parallel to Eqs. (17)–(19) we may define Yukawa matrices in the basis of mass eigenstates as $(f = u, d, l)$

$$\Pi_f \equiv V_f \Pi^0_f U^\dagger_f, \qquad \Sigma_f \equiv V_f \Sigma^0_f U^\dagger_f, \tag{26a}$$
$$\Gamma_f \equiv V_f \Gamma^0_f U^\dagger_f, \qquad \rho_f \equiv V_f \rho^0_f U^\dagger_f. \tag{26b}$$

Importantly, in the Higgs basis the Σ^0_f are diagonalized by the singular value decomposition involving V_f and U_f, but in general the ρ^0_f are not. This implies that Higgs-mediated FCNCs are induced by the coupling with the zero-VEV Higgs doublet $\Phi_\perp$.

From Eqs. (17)–(19), (23), and (25) we obtain

$$\Pi_f = \sqrt{2} \frac{M^D_f}{v} \sin\beta + \rho_f \cos\beta, \tag{27}$$

where $\Pi_f \equiv V_f \Pi^0_f U^\dagger_f$ and $\rho_f \equiv V_f \rho^0_f U^\dagger_f$. The ρ_f matrices contain non-zero off-diagonal components, which reflects that in general the two types of Yukawa coupling matrices

[3] The Σ^0 and ρ^0 matrices correspond to η and $\hat{\xi}$ in Ref. [42], see their Eq. (30).

Γ_f^0 and Π_f^0 can not be simultaneously diagonalized in the 2HDM. The ρ_f term in Eq. (27) can induce Higgs-mediated flavour-changing neutral currents (FCNC) at the tree-level. `GM2Calc` implements several variants of the 2HDM with or without Higgs-mediated FCNC:

- The four well-known types with Z_2 symmetry: type I, type II, type X, type Y,
- the flavour-aligned 2HDM (FA2HDM) [83,84], which also avoids tree-level Higgs-mediated FCNC and contains the four previous types as special cases,
- the 2HDM with general Yukawa structures.

We will now describe these variants of the 2HDM. The most common way to avoid FCNC is to impose a Z_2 symmetry, which leads to four different types of Yukawa interactions in which specific subsets of Yukawa couplings vanish. In the type I model all quarks and charged leptons couple to Φ_2, so we set

$$\Gamma_u^0 = \Gamma_d^0 = \Gamma_l^0 = 0. \tag{28}$$

In the type II model all up-type quarks couple to Φ_2, while the down-type quarks and charged leptons couple to Φ_1, so we set

$$\Gamma_u^0 = \Pi_d^0 = \Pi_l^0 = 0. \tag{29}$$

In the type X model all quarks couple to Φ_2, while the charged leptons couple to Φ_1, so we set

$$\Gamma_u^0 = \Gamma_d^0 = \Pi_l^0 = 0. \tag{30}$$

In the type Y model the up-type quarks and charged leptons couple to Φ_2, while the down-type quarks couple to Φ_1, so we set

$$\Gamma_u^0 = \Pi_d^0 = \Gamma_l^0 = 0. \tag{31}$$

In all these cases, trivially Γ_f^0 and Π_f^0 can be diagonalized simultaneously, and Higgs-mediated FCNC is avoided.

In the flavour-aligned Two-Higgs Doublet Model (FA2HDM) [83,84] it is assumed that the Π_f^0 matrices are proportional to the Γ_f^0 matrices, and we set

$$\Pi_f^0 = \begin{cases} \xi_u^* \Gamma_u^0, & \text{if } f = u, \\ \xi_{d,l} \Gamma_{d,l}^0, & \text{if } f = d, l, \end{cases} \quad \text{with} \quad \xi_f = \frac{\zeta_f + \tan\beta}{1 - \zeta_f \tan\beta}, \tag{32}$$

where ζ_f are the alignment parameters which are constrained by experimental results and used in phenomenological studies. Note that the aligned model contains the type I, II, X and Y models as special cases when the alignment parameters ζ_f take the values given in Table 1.

Table 1 Values of the alignment parameters ζ_f for different types of Two-Higgs Doublet Models

	Type I	Type II	Type X	Type Y
ζ_u	$\cot\beta$	$\cot\beta$	$\cot\beta$	$\cot\beta$
ζ_d	$\cot\beta$	$-\tan\beta$	$\cot\beta$	$-\tan\beta$
ζ_l	$\cot\beta$	$-\tan\beta$	$-\tan\beta$	$\cot\beta$

We can summarize the fundamental Yukawa coupling matrices ρ_f $(f = u, d, l)$ for the different 2HDM variants and in different parametrizations as follows:

$$\rho_f = \begin{cases} \frac{\sqrt{2} M_f^D}{v} \zeta_f^{(*)} & \text{for type I, II, Y, Y} \\ & \text{(using Table 1)} \\ & \text{and for the exact FA2HDM,} \\ \frac{\sqrt{2} M_f^D}{v} \zeta_f^{(*)} + \Delta_f & \text{for the general 2HDM} \\ & \text{in FA2HDM parametrization,} \\ \frac{\Pi_f}{\cos\beta} - \frac{\sqrt{2} M_f^D}{v} \tan\beta & \text{for the general 2HDM} \\ & \text{in } \Pi \text{ parametrization.} \end{cases} \tag{33}$$

Here the ζ_f are the parameters introduced in Eq. (32) and Table 1, and the $(*)$ notation indicates the conjugate is present for the case $f = u$ and not present for $f = d, l$. `GM2Calc` offers two parametrizations for the general 2HDM. The "FA2HDM parametrization" starts from the FA2HDM and allows to directly modify the ρ_f by additional matrices Δ_f, which represents the deviation from the flavour-aligned (or type I, II, X, Y) limit. The second "Π parametrization" starts from Eq. (27) and allows to directly specify the fundamental Yukawa matrices Π_f.

After suitable unitary transformations, the Yukawa interaction in the Lagrangian of Eq. (13) takes the following form:

$$\begin{aligned} -\mathcal{L}_{\text{Yuk,int}} = {} & H^+ \left[\bar{u} \left(y_d^{H^\pm} P_R + y_u^{H^\pm} P_L \right) d + \bar{\nu} y_l^{H^\pm} P_R l \right] \\ & + \sum_{f=u,d,l} \left(\sum_{S=h,H} S \bar{f} y_f^S P_R f - \mathrm{i} A \bar{f} y_f^A P_R f \right) \\ & + \text{h. c.,} \end{aligned} \tag{34}$$

with the CKM matrix $V_{\text{CKM}} = V_u V_d^\dagger$ and the fermion mass eigenstates $f = f_L + f_R$, $(f = u, d, l)$, defined in Eq. (20).

The coupling matrices y_f^S are defined as [102]:

$$y_f^h = \frac{M_f^D}{v}\sin(\beta-\alpha) + \frac{\rho_f}{\sqrt{2}}\cos(\beta-\alpha), \tag{35}$$

$$y_f^H = \frac{M_f^D}{v}\cos(\beta-\alpha) - \frac{\rho_f}{\sqrt{2}}\sin(\beta-\alpha), \tag{36}$$

$$y_f^A = \begin{cases} \frac{\rho_u}{\sqrt{2}} & \text{if } f = u, \\ -\frac{\rho_{d,l}}{\sqrt{2}} & \text{if } f = d, l, \end{cases} \tag{37}$$

and the coupling between the charged Higgs and each of the fermions is:

$$y_f^{H^\pm} = \begin{cases} -\rho_u^\dagger V_{\text{CKM}} & \text{if } f = u, \\ V_{\text{CKM}}\rho_d & \text{if } f = d, \\ \rho_l & \text{if } f = l, \end{cases} \tag{38}$$

where ρ_f is given in Eq. (33).

2.2 Implemented contributions to a_μ

Relevant 2HDM contributions to a_μ arise at the one-loop and the two-loop level. The one-loop contributions are suppressed by two additional powers of the muon Yukawa coupling and thus of $\mathcal{O}(m_\mu^4)$; they are typically subleading unless some of the non-SM-like Higgs bosons have very small mass around a few GeV. The two-loop contributions can be classified into fermionic and bosonic contributions. They arise at the $\mathcal{O}(m_\mu^2)$ and are typically dominant. An important subclass of two-loop contributions are the so-called Barr–Zee diagrams, which contain a $\gamma\gamma$-Higgs one-loop subdiagram. These diagrams have been studied extensively [140–144] and fully calculated in Ref. [100]. The full set of two-loop bosonic and fermionic diagrams (at $\mathcal{O}(m_\mu^2)$) has been computed in Ref. [102] (see also Ref. [103] for further phenomenological discussions of the individual contributions). `GM2Calc` implements the full set of one-loop BSM contributions $a_\mu^{1\ell}$ of $\mathcal{O}(m_\mu^4)$ and the two-loop BSM contributions $a_\mu^{2\ell}$ of $\mathcal{O}(m_\mu^2)$ in the 2HDM from Ref. [102]. The full BSM contribution in the 2HDM (i.e. the difference between the 2HDM and the SM contributions) calculated by `GM2Calc` is therefore the sum

$$a_\mu^{\text{BSM}} = a_\mu^{1\ell} + a_\mu^{2\ell}. \tag{39}$$

In the following subsections we provide the explicit analytic results implemented in `GM2Calc`.

2.2.1 One-loop contributions

The one-loop BSM contributions to $a_\mu^{1\ell}$ in the 2HDM is of $\mathcal{O}(m_\mu^4)$ and are given by

$$\begin{aligned} a_\mu^{1\ell} = \frac{1}{8\pi^2}\Bigg\{ \sum_{i=1}^{3} \Bigg[\sum_{S=h,H,A} \frac{m_\mu^2}{m_S^2} A_S(i, m_l, m_S^2, y_l^S) \\ + \frac{m_\mu^2}{m_{H^\pm}^2} A_{H^\pm}(i, 0, m_{H^\pm}^2, y_l^{H^\pm}) \Bigg] \\ - \frac{m_\mu^2}{m_{h_{\text{SM}}}^2} A_h(2, m_l, m_{h_{\text{SM}}}^2, \mathbb{1}) \Bigg\}, \end{aligned} \tag{40}$$

with $m_l = (m_e, m_\mu, m_\tau)$, $m_\nu = (m_{\nu_e}, m_{\nu_\mu}, m_{\nu_\tau})$ and

$$A_h(i, m_l, m_S^2, y_l^S) = A_S^+(i, m_l, m_S^2, y_l^S), \tag{41}$$

$$A_H(i, m_l, m_S^2, y_l^S) = A_S^+(i, m_l, m_S^2, y_l^S), \tag{42}$$

$$A_A(i, m_l, m_S^2, y_l^S) = A_S^-(i, m_l, m_S^2, y_l^S),$$

$$A_S^\pm(i, m_l, m_S^2, y_l^S)$$

$$= \frac{1}{24}\left(\left|(y_l^S)_{i2}\right|^2 + \left|(y_l^S)_{2i}\right|^2\right) F_1^C\left(\frac{(m_l)_i^2}{m_S^2}\right) \tag{43}$$

$$\pm \frac{1}{3}\Re\mathfrak{e}\left[(y_l^S)_{i2}^*(y_l^S)_{2i}^*\right]\frac{(m_l)_i}{m_\mu} F_2^C\left(\frac{(m_l)_i^2}{m_S^2}\right), \tag{44}$$

$$A_{H^\pm}(i, m_\nu, m_S^2, y_l^S)$$

$$= -\frac{1}{48}\left|(y_l^S)_{i2}\right|^2 \left[F_1^N\left(\frac{m_{\nu_\mu}^2}{m_S^2}\right) + F_1^N\left(\frac{(m_\nu)_i^2}{m_S^2}\right)\right]. \tag{45}$$

Note, that the one-loop contribution from the SM Higgs boson h_{SM} is subtracted in Eq. (40) and is therefore not included in $a_\mu^{1\ell}$. The loop functions F_1^C, F_2^C and F_1^N are given by

$$\begin{aligned} F_1^C(x) &= \frac{2}{(x-1)^4}\left(2 + 3x - 6x^2 + x^3 + 6x\ln x\right), \\ F_1^C(0) &= 4,\ F_1^C(1) = 1, \end{aligned} \tag{46}$$

$$\begin{aligned} F_2^C(x) &= \frac{3}{2(1-x)^3}\left(-3 + 4x - x^2 - 2\ln x\right), \\ F_2^C(1) &= 1,\ F_2^C(\infty) = 0, \end{aligned} \tag{47}$$

$$\begin{aligned} F_1^N(x) &= \frac{2}{(x-1)^4}\left(1 - 6x + 3x^2 + 2x^3 - 6x^2\ln x\right), \\ F_1^N(0) &= 2,\ F_1^N(1) = 1,\ F_1^N(\infty) = 0. \end{aligned} \tag{48}$$

2.2.2 Two-loop contributions

The two-loop contributions of $\mathcal{O}(m_\mu^2)$ are divided into fermionic and bosonic loop contributions according to Ref. [102] as

$$a_\mu^{2\ell} = a_\mu^{\rm B} + a_\mu^{\rm F}, \tag{49}$$

where the very small contribution from the shift of the Fermi constant, $a_\mu^{\Delta r\text{-shift}}$, is neglected. We generalize the fermionic two-loop contributions from Ref. [102] in the general 2HDM to the case of CKM mixing as follows:

$$a_\mu^{\rm F} = a_\mu^{\rm F,N} + a_\mu^{\rm F,C}, \tag{50}$$

$$a_\mu^{\rm F,N} = \sum_{f=u,d,l}\sum_{i=1}^{3} \frac{\alpha_{\rm em}^2 m_\mu^2}{4\pi^2 m_W^2 s_W^2} \times \left[\sum_{S=h,H,A} f_f^S(m_S,(m_f)_i)\frac{\Re\mathfrak{e}\left[(y_f^S)_{ii}^*(y_l^S)_{22}\right]v^2}{(m_f)_i m_\mu} - f_f^{h_{\rm SM}}(m_{h_{\rm SM}},(m_f)_i)\right], \tag{51}$$

$$f_f^S(m_S,m_f) = q_f^2 N_f^c \frac{m_f^2}{m_S^2}\mathcal{F}_S(m_S,m_f) - q_f N_f^c \frac{g_v^l g_v^f}{s_W^2 c_W^2}\frac{m_f^2}{m_S^2-m_Z^2} \times \left[\mathcal{F}_S(m_S,m_f)-\mathcal{F}_S(m_Z,m_f)\right], \tag{53}$$

$$\mathcal{F}_S(m_S,m_f) = \begin{cases} -2+\ln\left(\frac{m_S^2}{m_f^2}\right)-\left(\frac{m_S^2-2m_f^2}{m_S^2}\right)\frac{\Phi(m_S,m_f,m_f)}{m_S^2-4m_f^2}, & S=h,H,h_{\rm SM},\\ \frac{\Phi(m_S,m_f,m_f)}{m_S^2-4m_f^2}, & S=A, \end{cases} \tag{54}$$

where $N_f^c = (1,3,3)$, $g_v^f = T_f^3/2 - s_W^2 q_f$, $T_f^3 = (-1/2,-1/2,1/2)$ and $q_f = (-1,-1/3,2/3)$ for $f = (l,d,u)$. The loop function $f_f^{H^\pm}$ is defined as:

$$f_f^{H^\pm}(m_{H^\pm},m_f,m_{f'}) = \begin{cases} \frac{m_l^2}{m_{H^\pm}^2-m_W^2}\left[\mathcal{F}_l^{H\pm}\left(\frac{m_l^2}{m_{H^\pm}^2}\right)-\mathcal{F}_l^{H^\pm}\left(\frac{m_l^2}{m_W^2}\right)\right], & f=l,\ f'=\nu,\\ 3\frac{m_d^2}{m_{H^\pm}^2-m_W^2}\left[\mathcal{F}_d^{H\pm}\left(\frac{m_d^2}{m_{H^\pm}^2},\frac{m_u^2}{m_{H^\pm}^2}\right)-\mathcal{F}_d^{H^\pm}\left(\frac{m_d^2}{m_W^2},\frac{m_u^2}{m_W^2}\right)\right], & f=d,\ f'=u,\\ 3\frac{m_u^2}{m_{H^\pm}^2-m_W^2}\left[\mathcal{F}_u^{H\pm}\left(\frac{m_d^2}{m_{H^\pm}^2},\frac{m_u^2}{m_{H^\pm}^2}\right)-\mathcal{F}_u^{H^\pm}\left(\frac{m_d^2}{m_W^2},\frac{m_u^2}{m_W^2}\right)\right], & f=u,\ f'=d, \end{cases} \tag{55}$$

$$a_\mu^{\rm F,C} = \sum_{i,j=1}^{3}\frac{\alpha_{\rm em}^2 m_\mu^2}{32\pi^2 m_W^2 s_W^4} \times \Bigg[f_u^{H^\pm}(m_{H^\pm},(m_u)_i,(m_d)_j) \times \frac{\Re\mathfrak{e}\left[(y_u^{H^\pm})_{ij}^*(V_{\rm CKM})_{ij}(y_l^{H^\pm})_{22}\right]v^2}{2(m_u)_i m_\mu} + f_d^{H^\pm}(m_{H^\pm},(m_d)_j,(m_u)_i) \times \frac{\Re\mathfrak{e}\left[(y_d^{H^\pm})_{ij}^*(V_{\rm CKM})_{ij}(y_l^{H^\pm})_{22}\right]v^2}{2(m_d)_j m_\mu} + f_l^{H^\pm}(m_{H^\pm},(m_l)_i,0)\frac{\Re\mathfrak{e}\left[(y_l^{H^\pm})_{ij}^*\delta_{ij}(y_l^{H^\pm})_{22}\right]v^2}{2(m_l)_i m_\mu}\Bigg]. \tag{52}$$

Note, that the two-loop contribution from the SM Higgs boson $h_{\rm SM}$ is subtracted in Eq. (51) and is therefore not included in $a_\mu^{2\ell}$. The loop functions f_f^S ($S=h,H,A,h_{\rm SM}$) are defined as:

where f_j' is the $SU(2)_L$ partner of generation j of the fermion f_i from generation i, and

$$\mathcal{F}_l^{H^\pm}(x_l) = x_l + x_l(x_l-1)\left[{\rm Li}_2\left(1-\frac{1}{x_l}\right)-\frac{\pi^2}{6}\right] + \left(x_l-\frac{1}{2}\right)\ln(x_l), \tag{56}$$

$$\mathcal{F}_d^{H^\pm}(x_d,x_u) = -(x_u+x_d)+\left[\frac{\bar{c}}{y}-\frac{c(x_u-x_d)}{y}\right] \times \Phi(x_d,x_u,1) + c\left[{\rm Li}_2(1-x_d/x_u)-\frac{1}{2}\ln(x_u)\ln(x_d/x_u)\right] + (s+x_d)\ln(x_d)+(s-x_u)\ln(x_u), \tag{57}$$

$$\mathcal{F}_u^{H^\pm}(x_d,x_u) = \mathcal{F}_d^{H^\pm}(x_d,x_u)(q_u\to 2+q_u,\ q_d\to 2+q_d) - \frac{4}{3}\frac{(x_u-x_d-1)}{y}\Phi(x_d,x_u,1) - \frac{1}{3}\left[\ln^2(x_d)-\ln^2(x_u)\right], \tag{58}$$

and

$$c = (x_u - x_d)^2 - q_u x_u + q_d x_d, \tag{59}$$

$$\overline{c} = (x_u - q_u)x_u - (x_d + q_d)x_d, \tag{60}$$

$$y = (x_u - x_d)^2 - 2(x_u + x_d) + 1, \tag{61}$$

$$s = \frac{q_u + q_d}{4}. \tag{62}$$

The loop function $\Phi(m_1^2, m_2^2, m_3^2)$ [145] is defined as:

$$\Phi(m_1^2, m_2^2, m_3^2) = \frac{\lambda}{2}\Bigg[2\ln(\alpha_+)\ln(\alpha_-) - \ln\left(\frac{m_1^2}{m_3^2}\right)\ln\left(\frac{m_2^2}{m_3^2}\right) - 2\,\mathrm{Li}_2(\alpha_+) - 2\,\mathrm{Li}_2(\alpha_-) + \frac{\pi^2}{3}\Bigg], \tag{63}$$

$$\alpha_\pm = \frac{m_3^2 \pm m_1^2 \mp m_2^2 - \lambda}{2m_3^2}, \tag{64}$$

$$\lambda = \sqrt{m_1^4 + m_2^4 + m_3^4 - 2m_1^2m_2^2 - 2m_2^2m_3^2 - 2m_3^2m_1^2}. \tag{65}$$

The bosonic two-loop contributions to the general 2HDM are composed of three parts as follows:

$$a_\mu^{\mathrm{B}} = a_\mu^{\mathrm{B,EW\ add}} + a_\mu^{\mathrm{B,Yuk}} + a_\mu^{\mathrm{B,non\text{-}Yuk}}. \tag{66}$$

The two terms $a_\mu^{\mathrm{B,EW\ add}}$ and $a_\mu^{\mathrm{B,nonYuk}}$ correspond to diagrams with the SM-like Higgs boson and diagrams without the new Yukawa couplings, respectively. They are typically subdominant, and full details on their definition and phenomenological impact are given in Refs. [102,103]. The Yukawa contribution is given by

$$\begin{aligned} a_\mu^{\mathrm{B,Yuk}} = \frac{\alpha_{\mathrm{em}}^2}{574\pi^2 c_W^4 s_W^4}\frac{m_\mu^2}{m_Z^2} \Bigg\{ & a_{0,0}^0 + a_{0,z}^0\left(\tan\beta - \frac{1}{\tan\beta}\right)\zeta_l + a_{5,0}^0\Lambda_5 \\ & + a_{5,z}^0\left(\tan\beta - \frac{1}{\tan\beta}\right)\Lambda_{567}\zeta_l \\ & + \Bigg[a_{0,0}^1\left(\tan\beta - \frac{1}{\tan\beta}\right) + a_{0,z}^1\zeta_l \\ & + a_{5,0}^1\left(\tan\beta - \frac{1}{\tan\beta}\right)\Lambda_{567} \\ & + a_{5,z}^1\Lambda_5\zeta_l\Bigg]\cos(\beta-\alpha)\Bigg\}, \end{aligned} \tag{67}$$

$$\Lambda_5 = \frac{2m_{12}^2}{v^2\sin\beta\cos\beta}, \tag{68}$$

$$\Lambda_{567} = \Lambda_5 + \frac{1}{\tan\beta - \frac{1}{\tan\beta}}\left(\frac{\lambda_6}{\sin^2\beta} - \frac{\lambda_7}{\cos^2\beta}\right), \tag{69}$$

where the equations for $a_{\lambda,t}^\eta$ (with the common prefactor put in the front of the above Eq. (67)) are given in the appendix of Ref. [102]. Compared to this reference, the expression has been generalized to include λ_6 and λ_7.[4] These bosonic contributions are implemented in the realistic approximation of small $\cos(\beta-\alpha)$, and only terms up to linear order in $\cos(\beta-\alpha)$ are taken into account. In this scenario the boson h has the tree-level couplings of the SM Higgs boson [146]. Furthermore, the bosonic contributions are derived only for the flavour-aligned 2HDM. Referring to the different cases of Yukawa couplings in Eq. (33), the bosonic corrections apply for the cases of the discrete symmetries, for the FA2HDM, and also for the general 2HDM in FA2HDM parametrization (assuming the Δ_f matrices are small). In contrast, we set $\zeta_l = 0$ in Eq. (67) in the case of the general 2HDM in Π parametrization since in this case the bosonic corrections are not applicable in this form.

The bosonic two-loop contributions are also available in the `GM2Calc` source code and in the form of a `Mathematica` file.

2.2.3 Running couplings

Among the fermionic two-loop contributions, the diagrams with an internal top quark, bottom quark or tau lepton loop give the dominant contribution to a_μ^{BSM}. These diagrams are proportional to the values of the fermion masses in the loop. So long as there is no three-loop calculation available in the 2HDM, it is formally irrelevant which renormalization scheme to use for the fermion masses in the loop. In `GM2Calc` two possible definitions of these fermion masses are implemented:

[4] These two Higgs potential parameters only enter via triple Higgs couplings, and they enter only via the combination Λ_{567} defined in Eq. (69). The suitable generalizations of Eqs. (3.25)–(3.26) of Ref. [102] for the required triple Higgs couplings can be obtained e.g. from formulas in the Appendix of Ref. [146] and can simply be written as

$$g_{h,H^\pm,H^\mp} \propto \Bigg\{ v\left(\Lambda_5 - \frac{m_h^2}{v^2} - 2\frac{m_{H^\pm}^2}{v^2}\right) + \eta\left(\tan\beta - \frac{1}{\tan\beta}\right)\frac{v}{2}\left(2\frac{m_h^2}{v^2} - \Lambda_{567}\right)\Bigg\}, \tag{70}$$

$$g_{H,H^\pm,H^\mp} \propto \Bigg\{ \left(\tan\beta - \frac{1}{\tan\beta}\right)\frac{v}{2}\left(\Lambda_{567} - 2\frac{m_H^2}{v^2}\right) + \eta v\left(\Lambda_5 - \frac{m_H^2}{v^2} - 2\frac{m_{H^\pm}^2}{v^2}\right)\Bigg\}. \tag{71}$$

This structure clarifies the appearance of Λ_{567} in Eq. (67).

$$\text{Input masses:} \quad m_t, m_b^{\overline{\text{MS}}}(m_b^{\overline{\text{MS}}}), m_\tau \tag{72}$$

$$\text{Running masses:} \quad m_t^{\overline{\text{MS}}}(Q), m_b^{\overline{\text{MS}}}(Q), m_\tau^{\overline{\text{MS}}}(Q) \tag{73}$$

In the "input masses" scheme, the top quark pole mass m_t, the $\overline{\text{MS}}$ bottom quark mass in the SM with five active quark flavours, $m_b^{\overline{\text{MS}}}$, at the renormalization scale $Q = m_b^{\overline{\text{MS}}}$, and the tau lepton pole mass m_τ are used in the loops. These masses are typically used as input for spectrum generators [136,137]. In the "running masses" scheme, the running $\overline{\text{MS}}$ top quark mass $m_t^{\overline{\text{MS}}}(Q)$, the $\overline{\text{MS}}$ bottom quark mass $m_b^{\overline{\text{MS}}}(Q)$ and the $\overline{\text{MS}}$ tau lepton mass $m_\tau^{\overline{\text{MS}}}(Q)$ are used in the loops. The renormalization scale Q is set to the mass of the Higgs boson in the Feynman diagram. The "running masses" scheme is also used in `2HDMC` [113]. The difference between these two schemes is shown in Sect. 4.

2.2.4 Uncertainty estimate

We provide an uncertainty estimate for $a_\mu^{2\ell}$ as follows:

$$\delta a_\mu^{2\ell} = \delta a_\mu^{2\ell,\Delta r} + \delta a_\mu^{2\ell,m_\mu^4} + \delta a_\mu^{3\ell}, \tag{74}$$

where

$$\delta a_\mu^{2\ell,\Delta r} = 2 \times 10^{-12}, \tag{75}$$

$$\delta a_\mu^{2\ell,m_\mu^4} = \left| a_\mu^{1\ell}\ \Delta\alpha_{\text{em}} \right|, \tag{76}$$

$$\delta a_\mu^{3\ell} = \left| a_\mu^{2\ell}\ \Delta\alpha_{\text{em}} \right|, \tag{77}$$

and

$$\Delta\alpha_{\text{em}} = -\frac{4\alpha_{\text{em}}}{\pi} \ln\left(\frac{m_{\text{NP}}}{m_\mu}\right), m_{\text{NP}} = \min\{m_H, m_A, m_{H^\pm}\}. \tag{78}$$

The term $\delta a_\mu^{2\ell,\Delta r}$ accounts for the fact that the two-loop contribution $a_\mu^{\Delta r\text{-shift}}$ has been neglected in Eq. (49). In Refs. [102,147] it was shown that in the relevant parameter space $|a_\mu^{\Delta r\text{-shift}}| \leq 2 \times 10^{-12}$, which we use as an upper bound in the uncertainty estimate. The term $\delta a_\mu^{2\ell,m_\mu^4}$ estimates missing two-loop terms of $\mathcal{O}(m_\mu^4)$ using the known universal two-loop QED logarithmic contributions [148]. The term $a_\mu^{3\ell}$ is an estimate for the expected three-loop contributions. From experience the QED contributions are among the largest contributions at each loop level. For this reason we use again the known universal logarithmic QED contributions from Ref. [148] to provide an estimate for the unknown three-loop contributions.

3 Program details and usage

3.1 Quick start

`GM2Calc` can be downloaded from https://gm2calc.hepforge.org/ or https://github.com/GM2Calc/GM2Calc, for example as[5]

```
wget --content-disposition \
  https://github.com/GM2Calc/GM2Calc/
archive/v2.0.0.tar.gz
tar -xf GM2Calc-2.0.0.tar.gz
cd GM2Calc-2.0.0
```

To build `GM2Calc` run the following commands:

```
mkdir build
cd build
cmake ..
make
```

To calculate a_μ^{BSM} in the 2HDM with `GM2Calc` from the command line, run

```
bin/gm2calc.x --thdm-input-file=../
input/example.thdm
```

Here, `example.thdm` is the name of the file that contains the input parameters.[6]

3.2 Requirements

To build `GM2Calc` the following programs and libraries are required:

- C++14 and C11 compatible compilers
- Eigen library, version 3.1 or higher [149] [http://eigen.tuxfamily.org]
- Boost library, version 1.37.0 or higher [150] [http://www.boost.org]
- (optional) `Wolfram Mathematica` or `Wolfram Engine` [151]
- (optional) `Python 2` or `Python 3` [152], using the package `cppyy` [153] [https://pypi.org/project/cppyy/]

3.3 Running `GM2Calc` from the command line

`GM2Calc` can be run from the command line with an SLHA-like [136,137] input file as

[5] To track changes made to `GM2Calc` and get automatic updates one may alternatively clone the `git` repository https://github.com/GM2Calc/GM2Calc

[6] For instructions and examples of running the MSSM evaluation see Ref. [135].

```
bin/gm2calc.x \
  --thdm-input-file=example.thdm
```

where `example.thdm` is the name of the SLHA-like input file. Alternatively, the input parameters can be piped in an SLHA-like format into `GM2Calc` as

```
cat example.thdm | bin/gm2calc.x \
  --thdm-input-file=-
```

The calculated value for a_μ^{BSM} and δa_μ is written to the standard output. Depending on the input options and parameters, the output may contain the following block with a_μ^{BSM} and δa_μ:

```
Block GM2CalcOutput
0     1.67323025E-11    # \
  Delta(g-2)_muon/2
1     3.36159655E-12    # \
  uncertainty of Delta(g-2)_muon/2
```

The SLHA-like format for the input parameters is defined in the following subsections.

3.3.1 General options

In the SLHA-like input the selection of the configuration flags for `GM2Calc` can be given in the `GM2CalcConfig` block as defined in Ref. [135]. An example `GM2CalcConfig` block reads as follows:

```
Block GM2CalcConfig
0     4     # output format (0 = \
  minimal, 1 = detailed,
#  2 = NMSSMTools, 3 = SPheno, 4 = \
  GM2Calc)
1     2     # loop order (0, 1 or 2)
2     1     # disable/enable \
  tan(beta) resummation (0 or 1)
3     0     # force output (0 or 1)
4     0     # verbose output (0 or \
  1)
5     1     # calculate \
  uncertainty (0 or 1)
6     1     # running couplings in \
  the THDM
```

The entry `GM2CalcConfig[0]` defines the output format. If `GM2CalcConfig[0] = 0`, a single number is printed to the `stdout`. This number is the value of a_μ^{BSM} or the uncertainty δa_μ, depending on the value of `GM2CalcConfig[5]`: If `GM2CalcConfig[5] = 0`, the value of a_μ^{BSM} is printed. If `GM2CalcConfig[5] = \ 1`, the value of δa_μ is printed. If `GM2CalcConfig[0] \ = 1`, a detailed output, suitable for debugging, is printed. If `GM2CalcConfig[0] = 2`, the value of a_μ^{BSM} is written to the output block entry `LOWEN[6]`. If `GM2CalcConfig[0] = 3`, the value of a_μ^{BSM} is written to the output block entry `SPhenoLowEnergy[21]`. If `GM2CalcConfig[0] = 4` (default), the value of a_μ^{BSM} is written to the output block entry `GM2CalcOutput[0]`.

The entry `GM2CalcConfig[1]` defines the loop order of the calculation, which can be set to `0`, `1` or `2`. The default value is `2` (recommended), which corresponds to the two-loop calculation of a_μ^{BSM}.

The entry `GM2CalcConfig[2]` disables/enables the resummation of $\tan\beta$ in the MSSM. By default $\tan\beta$ resummation is enabled, which corresponds to `GM2CalcConfig[2] = 1`. To disable $\tan\beta$ resummation, set `GM2CalcConfig[2] = 0`. When the calculation is performed in the 2HDM, the value of `GM2CalcConfig[2]` is ignored.

The next two options are useful for debugging. By setting the entry `GM2CalcConfig[3] = 1` (default: `0`), the output of `GM2Calc` can be forced, even if a physical problem (e.g. a tachyon) has occurred. Warning: If a physical problem has occurred, the output cannot be trusted. Forcing the output should only be used for debugging. By setting the entry `GM2CalcConfig[4] = 1` (default: `0`), additional information about the model parameters and the calculation is printed.

With the entry `GM2CalcConfig[5]` the calculation of the uncertainty δa_μ, c.f. Eq. (74), can be disabled/enabled (`0` or `1`).

The entry `GM2CalcConfig[6]` (default: `1`) is new in `GM2Calc` 2.0.0 and controls the definition of the fermion masses that are inserted into the fermionic two-loop contribution a_μ^{F}, see Sect. 2.2.3. If `GM2CalcConfig[6] = 0`, the input masses (72) are used. If `GM2CalcConfig[6] = \ 1`, the running masses (73) are used. The difference between these two schemes is shown in Sect. 4.

3.3.2 Standard Model input parameters

The Standard Model input parameters are read from the `SMINPUTS`, `GM2CalcInput` and `VCKMIN` blocks. Example blocks that define the Standard Model input parameters may read:

```
Block SMINPUTS
1      128.94579         # \
  alpha_em(MZ)^(-1) SM MS-bar
3      0.1184            # \
  alpha_s(MZ) SM MS-bar
4      91.1876           # MZ(pole)
5      4.18              # mb(mb) SM \
  MS-bar
6      173.34            # mtop(pole)
7      1.77684           # mtau(pole)
8      0                 # mnu3(pole)
9      80.385            # mW(pole)
11      0.000510998928    # \
  melectron(pole)
12      0                 # mnu1(pole)
13      0.1056583715      # \
  mmuon(pole)
14      0                 # mnu2(pole)
21      0.0047            # md(2 GeV)
22      0.0022            # mu(2 GeV)
23      0.096             # ms(2 GeV)
24      1.28              # mc(2 GeV)
Block GM2CalcInput
33      125.09            # SM Higgs \
  boson mass
Block VCKMIN                 # CKM \
  matrix in Wolfenstein \
  parametrization
1      0.2257            # lambda
2      0.814             # A
3      0.135             # rho-bar
4      0.349             # eta-bar
```

The entries of the SMINPUTS and VCKMIN are defined in Refs. [136,137]. In the block entry GM2CalcInput[33] the mass of the Standard Model Higgs boson can be given. Unset parameters in the SMINPUTS and GM2CalcInput blocks are assigned default values. Unset parameters in the VCKMIN block are assumed to be zero.

3.3.3 *Two-Higgs Doublet Model input parameters*

We allow the specification of the 2HDM input parameters in two different "bases", see Table 2. The basis parameters are defined as in [113]. In the "gauge basis" the Lagrangian parameters, $\lambda_{1,\ldots,7}$ are used as input. In the "mass basis" the Higgs boson masses and the mixing parameter $\sin(\beta-\alpha)$ are used as input, instead of the Lagrangian parameters $\lambda_{1,\ldots,5}$, but λ_6 and λ_7 can still be used. All available input parameters are listed in Table 3.

Mass basis input parameters The "mass basis" input parameters are read from the MINPAR and MASS blocks for compatibility with 2HDMC [113]. The following shows an example input in the "mass basis" for the type II 2HDM:

```
Block MINPAR                       # \
  model parameters
3          3                     # \
  tan(beta)
16          0                     # \
  lambda_6
17          0                     # \
  lambda_7
18          40000                 # \
  m_{12}^2
20          0.999                 # \
  sin(beta - alpha)
21          0                     # \
  zeta_u (only used if Yukawa type \
  = 5)
22          0                     # \
  zeta_d (only used if Yukawa type \
  = 5)
23          0                     # \
  zeta_l (only used if Yukawa type \
  = 5)
24          2                     # \
  Yukawa type (1, 2, 3, 4, 5 = \
  aligned, 6 = general)
Block MASS                         # \
  Higgs masses
25          125                   # mh, \
  lightest CP-even Higgs
35          400                   # mH, \
  heaviest CP-even Higgs
36          420                   # mA, \
  CP-odd Higgs
37          440                   # mH+, \
  charged Higgs
```

Unset parameters in the MINPAR and MASS blocks are assumed to be zero, except for $\tan\beta$ which will raise an error. Entry 24 of the MINPAR is used to select the type of 2HDM. Specifically the integer values $1,\ldots,6$ for the Yukawa type correspond to: 1 = type I, 2 = type II, 3 = type X, 4 = type Y, 5 = Flavour-Aligned, 6 = general 2HDM. The input entries 21, 22, and 23 in the MINPAR block can be used to set the values of ζ_u, ζ_d and ζ_l in the Flavour-Aligned 2HDM, and are ignored for all other types. Additional blocks for the general case are described below.

Gauge basis input parameters Alternatively, the input can be given in the "gauge basis" in a format compatible with 2HDMC [113]. In the "gauge basis" the 2HDM parameters must be given in the MINPAR block. The available "gauge basis" input parameters are listed in Table 3. The following shows an example input in the "gauge basis":

Table 2 2HDM input parameters for different basis ($f = u, d, l$)

Basis	Input parameters
Gauge	$\lambda_1, \ldots, \lambda_7, \tan\beta, m_{12}^2, \zeta_f, \Delta_f, \Pi_f$
Mass	$m_h, m_H, m_A, m_{H^\pm}, \sin(\beta-\alpha), \lambda_6, \lambda_7, \tan\beta, m_{12}^2, \zeta_f, \Delta_f, \Pi_f$

Table 3 2HDM input parameters for the SLHA and `Mathematica` interface

Input parameter	SLHA entry	`Mathematica` symbol	Allowed values
Parameters specific to the gauge basis			
$\lambda_1, \ldots, \lambda_7$	`MINPAR[11]`, ..., `MINPAR[17]`	`lambda`	$\mathbb{R}$
Parameters specific to the mass basis			
λ_6	`MINPAR[16]`	`lambda6`	$\mathbb{R}$
λ_7	`MINPAR[17]`	`lambda7`	$\mathbb{R}$
$\sin(\beta-\alpha)$	`MINPAR[20]`	`sinBetaMinusAlpha`	$[-1, 1]$
$\{m_h, m_H\}$	`MASS[25],MASS[35]`	`Mhh`	$\{\mathbb{R}_{\geq 0}, \mathbb{R}_{\geq 0}\}$
m_A	`MASS[36]`	`MAh`	$\mathbb{R}_{\geq 0}$
$m_{H^\pm}$	`MASS[37]`	`MHp`	$\mathbb{R}_{\geq 0}$
Parameters common to both the gauge and mass basis			
Yukawa type	`MINPAR[24]`	`yukawaType`	$1, \ldots, 6$
$\tan\beta$	`MINPAR[3]`	`TB`	$\mathbb{R}_{>0}$
m_{12}^2	`MINPAR[18]`	`m122`	$\mathbb{R}$
ζ_u	`MINPAR[21]`	`zetau`	$\mathbb{R}$
ζ_d	`MINPAR[22]`	`zetad`	$\mathbb{R}$
ζ_l	`MINPAR[23]`	`zetal`	$\mathbb{R}$
Δ_u	`GM2CalcTHDMDeltauInput`	`Deltau`	$\mathbb{R}^{3\times 3}$
Δ_d	`GM2CalcTHDMDeltadInput`	`Deltad`	$\mathbb{R}^{3\times 3}$
Δ_l	`GM2CalcTHDMDeltalInput`	`Deltal`	$\mathbb{R}^{3\times 3}$
Π_u	`GM2CalcTHDMPiuInput`	`Piu`	$\mathbb{R}^{3\times 3}$
Π_d	`GM2CalcTHDMPidInput`	`Pid`	$\mathbb{R}^{3\times 3}$
Π_l	`GM2CalcTHDMPilInput`	`Pil`	$\mathbb{R}^{3\times 3}$

```
Block MINPAR                           # \
  model parameters in gauge basis
3           3                     # \
  tan(beta)
11          0.7                     # \
  lambda_1
12          0.6                     # \
  lambda_2
13          0.5                     # \
  lambda_3
14          0.4                     # \
  lambda_4
15          0.3                     # \
  lambda_5
16          0.2                     # \
  lambda_6
17          0.1                     # \
  lambda_7
18          40000                   # \
  m_{12}^2
21          0                       # \
  zeta_u (only used if Yukawa type \
  = 5)
22          0                       # \
  zeta_d (only used if Yukawa type \
  = 5)
23          0                       # \
  zeta_l (only used if Yukawa type \
  = 5)
24          2                       # \
  Yukawa type (1, 2, 3, 4, 5 = \
  aligned, 6 = general)
```

Two parametrizations for the general 2HDM are implemented, see Eq. (33). The first option is a deviation from the FA2HDM (or types I, II, X, Y), parametrized by the additional matrices Δ_f. Thus, after choosing Yukawa type = 1, ..., 5, i.e. type I, II, X, Y and FA2HDM, the matrices Δ_u, Δ_d and Δ_l can be optionally given in the following dedicated blocks:

```
Block GM2CalcTHDMDeltauInput
1 1   0                        # \
  Re(Delta_u(1,1))
1 2   0                        # \
  Re(Delta_u(1,2))
1 3   0                        # \
  Re(Delta_u(1,3))
2 1   0                        # \
  Re(Delta_u(2,1))
2 2   0                        # \
  Re(Delta_u(2,2))
2 3   0                        # \
  Re(Delta_u(2,3))
3 1   0                        # \
  Re(Delta_u(3,1))
3 2   0                        # \
  Re(Delta_u(3,2))
3 3   0                        # \
  Re(Delta_u(3,3))
Block GM2CalcTHDMDeltadInput
1 1   0                        # \
  Re(Delta_d(1,1))
1 2   0                        # \
  Re(Delta_d(1,2))
1 3   0                        # \
  Re(Delta_d(1,3))
2 1   0                        # \
  Re(Delta_d(2,1))
2 2   0                        # \
  Re(Delta_d(2,2))
2 3   0                        # \
  Re(Delta_d(2,3))
3 1   0                        # \
  Re(Delta_d(3,1))
3 2   0                        # \
  Re(Delta_d(3,2))
3 3   0                        # \
  Re(Delta_d(3,3))
Block GM2CalcTHDMDeltalInput
1 1   0                        # \
  Re(Delta_l(1,1))
1 2   0                        # \
  Re(Delta_l(1,2))
1 3   0                        # \
  Re(Delta_l(1,3))
2 1   0                        # \
  Re(Delta_l(2,1))
2 2   0.1                      # \
  Re(Delta_l(2,2))
2 3   0                        # \
  Re(Delta_l(2,3))
3 1   0                        # \
  Re(Delta_l(3,1))
3 2   0                        # \
  Re(Delta_l(3,2))
3 3   0                        # \
  Re(Delta_l(3,3))
```

The other option for the general 2HDM corresponds to the Π parametrization, implemented when setting Yukawa type = 6. In this case, the input parameters Δ_u, Δ_d and Δ_l are ignored and the real parts of the matrices Π_u, Π_d and Π_l can be given in the following dedicated blocks:

```
Block GM2CalcTHDMPiuInput
1 1   0                        # \
  Re(Pi_u(1,1))
1 2   0                        # \
  Re(Pi_u(1,2))
1 3   0                        # \
  Re(Pi_u(1,3))
2 1   0                        # \
  Re(Pi_u(2,1))
2 2   0                        # \
  Re(Pi_u(2,2))
2 3   0                        # \
  Re(Pi_u(2,3))
3 1   0                        # \
  Re(Pi_u(3,1))
3 2   0                        # \
  Re(Pi_u(3,2))
3 3   0                        # \
  Re(Pi_u(3,3))
Block GM2CalcTHDMPidInput
1 1   0                        # \
  Re(Pi_d(1,1))
1 2   0                        # \
  Re(Pi_d(1,2))
1 3   0                        # \
  Re(Pi_d(1,3))
2 1   0                        # \
  Re(Pi_d(2,1))
2 2   0                        # \
  Re(Pi_d(2,2))
2 3   0                        # \
  Re(Pi_d(2,3))
3 1   0                        # \
  Re(Pi_d(3,1))
3 2   0                        # \
  Re(Pi_d(3,2))
3 3   0                        # \
  Re(Pi_d(3,3))
Block GM2CalcTHDMPilInput
1 1   0                        # \
  Re(Pi_l(1,1))
1 2   0                        # \
  Re(Pi_l(1,2))
1 3   0                        # \
  Re(Pi_l(1,3))
2 1   0                        # \
  Re(Pi_l(2,1))
2 2   0.1                      # \
  Re(Pi_l(2,2))
2 3   0                        # \
  Re(Pi_l(2,3))
3 1   0                        # \
  Re(Pi_l(3,1))
3 2   0                        # \
  Re(Pi_l(3,2))
3 3   0                        # \
  Re(Pi_l(3,3))
```

The input parameters Π_u, Π_d and Π_l are ignored when choosing Yukawa type = 1, …, 5, i.e. type I, II, X, Y and FA2HDM.

The SLHA-like interface described so far is very convenient and intuitive to use and it does not require any prior knowledge of programming languages to run GM2Calc this way. The execution time for this is also very short, around 5 ms per point on current laptops.[7] Nevertheless even faster execution times and easy interfacing with other existing calculators and sampling algorithms are enabled through our C++ (0.05 ms), C (0.05 ms), Mathematica (0.5 ms) and Python (0.08 ms) interfaces. In the following subsections we describe how to use each of these interfaces.

3.4 Running GM2Calc from within C++

GM2Calc provides a C++ programming interface, which allows for calculating of a_μ^{BSM} in the 2HDM up to the two-loop level. The following C++ source code snippet shows a two-loop example calculation in the 2HDM of type II with input parameters defined in the "mass basis", see Table 2.

```
#include "gm2calc/gm2_1loop.hpp"
#include "gm2calc/gm2_2loop.hpp"
#include "gm2calc/gm2_uncertainty.hpp"
#include "gm2calc/gm2_error.hpp"
#include "gm2calc/THDM.hpp"

#include <cstdio>

int main()
{
   // define THDM parameters in the \
  mass basis
   gm2calc::thdm::Mass_basis basis;
   basis.yukawa_type = \
  gm2calc::thdm::Yukawa_type::type_2;
   basis.mh = 125; \
                                // \
  light CP-even Higgs mass
   basis.mH = 400; \
                                // \
  heavy CP-even Higgs mass
   basis.mA = 420; \
                                // \
  CP-odd Higgs mass
   basis.mHp = 440; \
                               // \
  charged Higgs mass
   basis.sin_beta_minus_alpha = \
  0.999;         // sin(beta - alpha)
   basis.lambda_6 = 0; \
                            // lambda_6
   basis.lambda_7 = 0; \
                            // lambda_7
   basis.tan_beta = 3; \
                            // tan(beta)
   basis.m122 = 40000; \
                            // m_{12}^2 \
  in GeV^2
   basis.zeta_u = 0; \
                              // zeta_u
   basis.zeta_d = 0; \
                              // zeta_d
   basis.zeta_l = 0; \
                              // zeta_l
   basis.Delta_u << 0, 0, 0, 0, 0, 0, \
  0, 0, 0; // Delta_u
   basis.Delta_d << 0, 0, 0, 0, 0, 0, \
  0, 0, 0; // Delta_d
   basis.Delta_l << 0, 0, 0, 0, 0, 0, \
  0, 0, 0; // Delta_l
   basis.Pi_u << 0, 0, 0, 0, 0, 0, \
  0, 0;    // Pi_u
   basis.Pi_d << 0, 0, 0, 0, 0, 0, \
  0, 0;    // Pi_d
   basis.Pi_l << 0, 0, 0, 0, 0, 0, \
  0, 0;    // Pi_l

   // define SM parameters
   gm2calc::SM sm;
   sm.set_alpha_em_mz(1.0/128.94579); \
  // electromagnetic coupling
   sm.set_mu(2, 173.34); \
             // top quark mass
   sm.set_mu(1, 1.28); \
               // charm quark mass
   sm.set_md(2, 4.18); \
               // bottom quark mass
   sm.set_ml(2, 1.77684); \
            // tau lepton mass

   // define options to customize the \
  calculation
   gm2calc::thdm::Config config;
   config.running_couplings = true; \
     // use running couplings

   try {
      // setup the THDM
      gm2calc::THDM model(basis, sm, \
  config);

      // calculate a_mu up to \
  (including) the 2-loop level
      const double amu = \
  gm2calc::calculate_amu_1loop(model)
                            + \
  gm2calc::calculate_amu_2loop(model);

      // calculate the uncertainty of \
  the 2-loop a_mu
      const double delta_amu =
        gm2calc::calculate_uncertainty_
          amu_2loop(model);

      std::printf("amu = %g +- %g\n", \
  amu, delta_amu);
   } catch (const gm2calc::Error& e) {
      std::printf("%s\n", e.what());
   }

   return 0;
}
```

This example source code can be compiled as follows (assuming GM2Calc has been compiled to a shared library libgm2calc.so on a UNIX-like operating system with g++ installed):

[7] Based a machine with an Intel(R) Core(TM) i7-5600U CPU @ 2.60 GHz processor.

```
g++ -I${GM2CALC_DIR}/include/ \
  -I${EIGEN_DIR} example.cpp \
  ${GM2CALC_DIR}/build/lib/libgm2calc.so
```

Here `example.cpp` is the file that contains the above listed source code. The variable `GM2CALC_DIR` contains the path to the `GM2Calc` root directory and `EIGEN_DIR` contains the path to the Eigen library header files. Running the created executable `a.out` yields

```
$ ./a.out
amu = 1.67323e-11 +- 3.3616e-12
```

In line 12 of the example source code an object of type `Mass_basis` is created, which contains the input parameters in the mass basis, see Table 2. The mass basis input parameters are set in lines 13–31. Note that the Yukawa type is set to type II in line 13, which implies that given values of ζ_f are ignored and internally fixed to the values given in Table 1. Additionally the inputs Π_f and Δ_f are unused for this type, and ignored. In line 34 an object of type `SM` is created that contains all SM input parameters. The SM input parameters are set to reasonable default values from the PDG [154]. In lines 35–39 the values for $\alpha_{\text{em}}(m_Z)$, m_t, $m_c^{\overline{\text{MS}}}(2\,\text{GeV})$, $m_b^{\overline{\text{MS}}}(m_b^{\overline{\text{MS}}})$ and m_τ are set to specific values. In line 42 an object of type `Config` is created, which contains the options to customize the calculation of a_μ^{BSM} and δa_μ. In line 43 the "running masses" scheme is chosen, see Sect. 2.2.3. In line 47 the 2HDM model is created, given the 2HDM and SM input parameters and the configuration options defined above. The value of $a_\mu^{\text{BSM}} = a_\mu^{1\ell} + a_\mu^{2\ell}$ is calculated in lines 50–51. The corresponding uncertainty δa_μ is calculated in line 54–55. The values a_μ^{BSM} and δa_μ are printed in line 57. Note that the 2HDM model should be created within a `try` block, because the constructor of the 2HDM class throws an exception if a physical problem occurs (e.g. a tachyon) or an input parameter has been set to an invalid value, see Table 3.

Alternatively, the 2HDM input parameters can be given in the "gauge basis", i.e. in terms of the Lagrangian parameters, see Table 2. The following C++ source code snippet shows a corresponding example two-loop calculation in the 2HDM of type II, where the input parameters are defined in the "gauge basis".

```
#include "gm2calc/gm2_1loop.hpp"
#include "gm2calc/gm2_2loop.hpp"
#include "gm2calc/gm2_uncertainty.hpp"
#include "gm2calc/gm2_error.hpp"
#include "gm2calc/THDM.hpp"

#include <cstdio>

int main()
{
   // define THDM parameters in the gauge \
  basis
 gm2calc::thdm::Gauge_basis basis;
 basis.yukawa_type = \
gm2calc::thdm::Yukawa_type::type_2;
 basis.lambda << 0.7, 0.6, 0.5, 0.4, \
0.3, 0.2, 0.1;   // lambda_{1,...,7}
 basis.tan_beta = 3; \
                                  // \
tan(beta)
 basis.m122 = 40000; \
                                  // \
m_{12}^2 in GeV^2
 basis.zeta_u = 0; \
                                    // \
zeta_u
 basis.zeta_d = 0; \
                                    // \
zeta_d
 basis.zeta_l = 0; \
                                    // \
zeta_l
 basis.Delta_u << 0, 0, 0, 0, 0, 0, 0, \
0, 0;          // Delta_u
 basis.Delta_d << 0, 0, 0, 0, 0, 0, 0, \
0, 0;          // Delta_d
 basis.Delta_l << 0, 0, 0, 0, 0, 0, 0, \
0, 0;          // Delta_l
 basis.Pi_u << 0, 0, 0, 0, 0, 0, 0, 0, \
0;             // Pi_u
 basis.Pi_d << 0, 0, 0, 0, 0, 0, 0, 0, \
0;             // Pi_d
 basis.Pi_l << 0, 0, 0, 0, 0, 0, 0, 0, \
0;             // Pi_l

 // define SM parameters
 gm2calc::SM sm;
 sm.set_alpha_em_mz(1.0/128.94579);   // \
electromagnetic coupling
 sm.set_mu(2, 173.34);                // \
top quark mass
 sm.set_mu(1, 1.28);                  // \
charm quark mass
 sm.set_md(2, 4.18);                  // \
bottom quark mass
 sm.set_ml(2, 1.77684);               // \
tau lepton mass

 // define options to customize the \
calculation
 gm2calc::thdm::Config config;
 config.running_couplings = true;     // \
use running couplings

 try {
    // setup the THDM
    gm2calc::THDM model(basis, sm, \
config);

    // calculate a_mu up to (including) \
the 2-loop level
    const double amu = \
gm2calc::calculate_amu_1loop(model)
                     + \
gm2calc::calculate_amu_2loop(model);

    // calculate the uncertainty of the \
2-loop a_mu
    const double delta_amu =
       gm2calc::calculate_uncertainty_
       amu_2loop(model);

    std::printf("amu = %g +- %g\n", \
amu, delta_amu);
 } catch (const gm2calc::Error& e) {
```

```
54         std::printf("%s\n", e.what());
55     }
56
57     return 0;
58 }
```

In line 12 an object of type `Gauge_basis` is created, which is filled with the gauge basis input parameters in lines 13–25. With the defined gauge basis input parameters the calculation of a_μ^{BSM} and δa_μ continues as in the mass basis example above.

3.5 Running `GM2Calc` from within C

Alternatively to the C++ programming interface detailed in Sect. 3.4, `GM2Calc` also provides a C programming interface. The following C source code snippet shows a two-loop example calculation in the 2HDM of type II with input parameters defined in the "mass basis", see Table 2.

```
#include "gm2calc/gm2_1loop.h"
#include "gm2calc/gm2_2loop.h"
#include "gm2calc/gm2_uncertainty.h"
#include "gm2calc/THDM.h"
#include "gm2calc/SM.h"

#include <stdio.h>

int main()
{
   /* define THDM parameters in the mass \
  basis */
   const gm2calc_THDM_mass_basis basis = {
      .yukawa_type = gm2calc_THDM_type_2, \
        /* Yukawa type */
      .mh = 125, \
                                 /* light \
  CP-even Higgs mass */
      .mH = 400, \
                                 /* heavy \
  CP-even Higgs mass */
      .mA = 420, \
                                 /* \
  CP-odd Higgs mass */
      .mHp = 440, \
                                /* \
  charged Higgs mass */
      .sin_beta_minus_alpha = 0.999, \
           /* sin(beta - alpha) */
      .lambda_6 = 0, \
                             /* lambda_6 */
      .lambda_7 = 0, \
                             /* lambda_7 */
      .tan_beta = 3, \
                             /* tan(beta) \
  */
      .m122 = 40000, \
                             /* m_{12}^2 \
  in GeV^2 */
      .zeta_u = 0, \
                               /* zeta_u */
      .zeta_d = 0, \
                               /* zeta_d */
      .zeta_l = 0, \
                               /* zeta_l */
      .Delta_u = { {0,0,0}, {0,0,0}, \
  {0,0,0} }, /* Re(Delta_u(i,k)) */
      .Delta_d = { {0,0,0}, {0,0,0}, \
  {0,0,0} }, /* Re(Delta_d(i,k)) */
      .Delta_l = { {0,0,0}, {0,0,0}, \
  {0,0,0} }, /* Re(Delta_l(i,k)) */
      .Pi_u = { {0,0,0}, {0,0,0}, {0,0,0} \
  },    /* Re(Pi_u(i,k)) */
      .Pi_d = { {0,0,0}, {0,0,0}, {0,0,0} \
  },    /* Re(Pi_d(i,k)) */
      .Pi_l = { {0,0,0}, {0,0,0}, {0,0,0} \
  }     /* Re(Pi_l(i,k)) */
   };

   /* define SM parameters */
   gm2calc_SM sm;
   gm2calc_sm_set_to_default(&sm);
   sm.alpha_em_mz = 1.0/128.94579;   /* \
  electromagnetic coupling */
   sm.mu[2] = 173.34;                /* \
  top quark mass */
   sm.mu[1] = 1.28;                  /* \
  charm quark mass */
   sm.md[2] = 4.18;                  /* \
  bottom quark mass */
   sm.ml[2] = 1.77684;               /* \
  tau lepton mass */

   /* calculation settings */
   gm2calc_THDM_config config;
   gm2calc_thdm_config_set_to_default
     (&config);

   /* setup the THDM */
   gm2calc_THDM* model = 0;
   gm2calc_error error = \
  gm2calc_thdm_new_with_mass_basis(&model, \
  &basis, &sm, &config);

   if (error == gm2calc_NoError) {
      /* calculate a_mu up to (including) \
  the 2-loop level */
      const double amu = \
  gm2calc_thdm_calculate_amu_1loop(model)
                     + \
  gm2calc_thdm_calculate_amu_2loop(model);

      /* calculate the uncertainty of the \
  2-loop a_mu */
      const double delta_amu =
         gm2calc_thdm_calculate_uncertainty_
           amu_2loop(model);

      printf("amu = %g +- %g\n", amu, \
  delta_amu);
   } else {
      printf("Error: %s\n", \
  gm2calc_error_str(error));
   }

   gm2calc_thdm_free(model);

   return 0;
}
```

This example source code can be compiled as follows (assuming `GM2Calc` has been compiled to a shared library `libgm2calc.so` on a UNIX-like operating system with `gcc` installed):

```
gcc -I${GM2CALC_DIR}/include/ \
  example.c \
  ${GM2CALC_DIR}/build/lib/ \
  libgm2calc.so
```

Here `example.c` is the file that contains the above listed source code.

The C example source code is very similar to the mass basis C++ example. In line 12 an object of type `gm2calc_THDM_mass_basis` is created and filled with the mass basis input parameters in lines 13–32. The Yukawa type of the model is defined in line 13 to be type II. In line 35 an object of type `gm2calc_SM` is created, which contains the SM input parameters. The SM input parameters are set to their default values in line 36. In lines 37–41 the values of $\alpha_{\text{em}}(m_Z)$, m_t, $m_c^{\overline{\text{MS}}}(2\,\text{GeV})$, $m_b^{\overline{\text{MS}}}(m_b^{\overline{\text{MS}}})$ and m_τ are set to specific values. In line 44 a config object of type `gm2calc_THDM_config` is created which contains options to customize the calculation. These options are set to default values in line 45. In line 48 a null-pointer to a 2HDM model of type `gm2calc_THDM` is created. In line 49 the 2HDM model is created and the pointer is set to point to the model. If an error occurrs, the pointer is set to 0 and the returned `error` variable is set to a value that is not `gm2calc_NoError`. If no error has occurred, the example continues to calculate a_μ^{BSM} and δa_μ in lines 53–58, respectively. The result is printed in line 60. In line 65 the memory reserved for the 2HDM model is freed.

Alternatively, the 2HDM input parameters can be given in the "gauge basis", similarly to the gauge basis C++ example. The following C source code snippet shows a corresponding example two-loop calculation in the 2HDM of type II, where the input parameters are defined in the "gauge basis".

```
1  #include "gm2calc/gm2_1loop.h"
2  #include "gm2calc/gm2_2loop.h"
3  #include "gm2calc/gm2_uncertainty.h"
4  #include "gm2calc/THDM.h"
5  #include "gm2calc/SM.h"
6
7  #include <stdio.h>
8
9  int main()
10 {
11    /* define THDM parameters in the gauge \
   basis */
12    const gm2calc_THDM_gauge_basis basis = {
13       .yukawa_type = gm2calc_THDM_type_2, \
                /* Yukawa type */
14       .lambda = { 0.7, 0.6, 0.5, 0.4, \
   0.3, 0.2, 0.1 }, /* lambda_i */
15       .tan_beta = 3, \
                                    /* \
   tan(beta) */
16       .m122 = 40000, \
                                    /* \
   m_{12}^2 in GeV^2 */
17       .zeta_u = 0, \
                                      /* \
   zeta_u */
18       .zeta_d = 0, \
                                      /* \
   zeta_d */
19       .zeta_l = 0, \
                                      /* \
   zeta_l */
20       .Delta_u = { {0,0,0}, {0,0,0}, \
   {0,0,0} },          /* Re(Delta_u(i,k)) */
21       .Delta_d = { {0,0,0}, {0,0,0}, \
   {0,0,0} },          /* Re(Delta_u(i,k)) */
22       .Delta_l = { {0,0,0}, {0,0,0}, \
   {0,0,0} },          /* Re(Delta_u(i,k)) */
23       .Pi_u = { {0,0,0}, {0,0,0}, {0,0,0} \
   },          /* Re(Pi_u(i,k)) */
24       .Pi_d = { {0,0,0}, {0,0,0}, {0,0,0} \
   },          /* Re(Pi_d(i,k)) */
25       .Pi_l = { {0,0,0}, {0,0,0}, {0,0,0} \
   }           /* Re(Pi_l(i,k)) */
26    };
27
28    /* define SM parameters */
29    gm2calc_SM sm;
30    gm2calc_sm_set_to_default(&sm);
31    sm.alpha_em_mz = 1.0/128.94579;   /* \
   electromagnetic coupling */
32    sm.mu[2] = 173.34;                /* \
   top quark mass */
33    sm.mu[1] = 1.28;                  /* \
   charm quark mass */
34    sm.md[2] = 4.18;                  /* \
   bottom quark mass */
35    sm.ml[2] = 1.77684;               /* \
   tau lepton mass */
36
37    /* calculation settings */
38    gm2calc_THDM_config config;
39    gm2calc_thdm_config_set_to_default(&config);
40
41    /* setup the THDM */
42    gm2calc_THDM* model = 0;
43    gm2calc_error error = \
   gm2calc_thdm_new_with_gauge_basis(&model, \
   &basis, &sm, &config);
44
45    if (error == gm2calc_NoError) {
46       /* calculate a_mu up to (including) \
   the 2-loop level */
47       const double amu = \
   gm2calc_thdm_calculate_amu_1loop(model)
48                        + \
   gm2calc_thdm_calculate_amu_2loop(model);
49
50       /* calculate the uncertainty of the \
   2-loop a_mu */
51       const double delta_amu =
52          gm2calc_thdm_calculate_uncertainty_
53          amu_2loop(model);
54
55       printf("amu = %g +- %g\n", amu, \
   delta_amu);
56    } else {
57       printf("Error: %s\n", \
   gm2calc_error_str(error));
58    }
59
60    gm2calc_thdm_free(model);
61
62    return 0;
63 }
```

In line 12 an object of type `gm2calc_THDM_gauge_basis` is created, which is filled with the gauge basis input parameters in lines 13–26. In line 43 the 2HDM model is created, using the gauge basis input parameters. The calculation of a_μ^{BSM} and δa_μ is performed in lines 47–52, as in the "mass basis" example above.

3.6 Running `GM2Calc` from within `Mathematica`

`GM2Calc` can be run from within `Mathematica` using the `MathLink` interface. The following source code snippet shows an example calculation of a_μ^{BSM} and its uncertainty at the two-loop level using input parameters given in the "gauge basis".

```
1  Install["bin/gm2calc.mx"];
2
3  (* calculation settings *)
4  GM2CalcSetFlags[
5      loopOrder -> 2,
6      runningCouplings -> True];
7
8  (* set SM parameters *)
9  GM2CalcSetSMParameters[
10     alpha0 -> 0.00729735,        (* \
     alpha_em in Thompson limit *)
11     alphaMZ -> 0.0077552,        (* \
     alpha_em(MZ) *)
12     alphaS -> 0.1184,            (* alpha_s \
     *)
13     MhSM -> 125.09,              (* SM \
     Higgs boson pole mass *)
14     MW -> 80.385,                (* W boson \
     pole mass *)
15     MZ -> 91.1876,               (* Z boson \
     pole mass *)
16     MT -> 173.34,                (* top \
     quark pole mass *)
17     mcmc -> 1.28,                (* charm \
     quark MS-bar mass mc at Q = mc *)
18     mu2GeV -> 0.0022,            (* up \
     quark MS-bar mass at Q = 2 GeV *)
19     mbmb -> 4.18,                (* bottom \
     quark MS-bar mass mb at Q = mb *)
20     ms2GeV -> 0.096,             (* strange \
     quark MS-bar mass at Q = 2 GeV *)
21     md2GeV -> 0.0047,            (* down \
     quark MS-bar mass at Q = 2 GeV *)
22     ML -> 1.777,                 (* tau \
     lepton pole mass *)
23     MM -> 0.1056583715,          (* muon \
     pole mass *)
24     ME -> 0.000510998928,        (* \
     electron pole mass *)
25     Mv1 -> 0,                    (* \
     lightest neutrino mass *)
26     Mv2 -> 0,                    (* 2nd \
     lightest neutrino mass *)
27     Mv3 -> 0,                    (* \
     heaviest neutrino mass *)
28     CKM -> IdentityMatrix[3]     (* CKM \
     matrix *)
29 ];
30
31 (* calculate amu using the gauge basis \
     input parameters *)
32 result = {amu, Damu} /. \
     GM2CalcAmuTHDMGaugeBasis[
33     yukawaType          -> 2, \
                         (* Yukawa type \
     (1,...,6) *)
34     lambda              -> { 0.7, 0.6, 0.5, \
     0.4, 0.3, 0.2, 0.1 }, (* \
     lambda_{1,...,7} *)
35     TB                  -> 3, \
                           (* tan(beta) = v2/v1 \
     *)
36     m122                -> 200^2, \
                         (* m_{12}^2 *)
37     zetau               -> 0, \
                           (* zeta_u *)
38     zetad               -> 0, \
                           (* zeta_d *)
39     zetal               -> 0, \
                           (* zeta_l *)
40     Deltau              -> 0 \
     IdentityMatrix[3],    (* Delta_u *)
41     Deltad              -> 0 \
     IdentityMatrix[3],    (* Delta_d *)
42     Deltal              -> 0 \
     IdentityMatrix[3],    (* Delta_l *)
43     Piu                 -> 0 \
     IdentityMatrix[3],    (* Pi_u *)
44     Pid                 -> 0 \
     IdentityMatrix[3],    (* Pi_d *)
45     Pil                 -> 0 \
     IdentityMatrix[3]     (* Pi_l *)
46     ];
47
48 Print[result];
```

In line 1 `GM2Calc`'s `MathLink` executable `bin/gm2calc.mx`, which is created when building `GM2Calc`, is loaded into the `Mathematica` session. In lines 4–6 two configuration options to customize the calculation are set: The calculation shall be performed at the two-loop level using the "running masses" scheme defined in Sect. 2.2.3. In lines 9–29 the SM input parameters are defined. Unset parameters are set to reasonable default values, see `Options[GM2CalcSetSMParameters]`. In lines 32–46 the values of a_μ^{BSM} and δa_μ are calculated using the function `GM2CalcAmuTHDMGaugeBasis`, which takes the gauge basis input parameters as arguments, see Table 3. The result is printed in line 48.

Alternatively, the calculation can be performed using input parameters given in the "mass basis". The following source code snippet shows an example calculation of a_μ^{BSM} and its uncertainty at the two-loop level using input parameters given in the "mass basis".

```
Install["bin/gm2calc.mx"];

(* calculation settings *)
GM2CalcSetFlags[
    loopOrder -> 2,
    runningCouplings -> True];

(* set SM parameters *)
GM2CalcSetSMParameters[
    alpha0 -> 0.00729735,        (* \
  alpha_em in Thompson limit *)
    alphaMZ -> 0.0077552,        (* \
  alpha_em(MZ) *)
    alphaS -> 0.1184,            (* alpha_s \
  *)
```

```
13   MhSM -> 125.09,              (* SM \
   Higgs boson pole mass *)
14   MW -> 80.385,                (* W boson \
   pole mass *)
15   MZ -> 91.1876,               (* Z boson \
   pole mass *)
16   MT -> 173.34,                (* top \
   quark pole mass *)
17   mcmc -> 1.28,                (* charm \
   quark MS-bar mass mc at Q = mc *)
18   mu2GeV -> 0.0022,            (* up \
   quark MS-bar mass at Q = 2 GeV *)
19   mbmb -> 4.18,                (* bottom \
   quark MS-bar mass mb at Q = mb *)
20   ms2GeV -> 0.096,             (* strange \
   quark MS-bar mass at Q = 2 GeV *)
21   md2GeV -> 0.0047,            (* down \
   quark MS-bar mass at Q = 2 GeV *)
22   ML -> 1.777,                 (* tau \
   lepton pole mass *)
23   MM -> 0.1056583715,          (* muon \
   pole mass *)
24   ME -> 0.000510998928,        (* \
   electron pole mass *)
25   Mv1 -> 0,                    (* \
   lightest neutrino mass *)
26   Mv2 -> 0,                    (* 2nd \
   lightest neutrino mass *)
27   Mv3 -> 0,                    (* \
   heaviest neutrino mass *)
28   CKM -> IdentityMatrix[3]     (* CKM \
   matrix *)
29 ];
30
31 (* calculate amu using the mass basis \
   input parameters *)
32 result = {amu, Damu} /. \
   GM2CalcAmuTHDMMassBasis[
33   yukawaType          -> 2, \
                      (* Yukawa type \
   (1,...,6) *)
34   Mhh                 -> { 125, 400 }, \
           (* CP-even Higgs boson masses *)
35   MAh                 -> 420, \
                 (* CP-odd Higgs boson \
   mass *)
36   MHp                 -> 440, \
                 (* charged Higgs boson \
   mass *)
37   sinBetaMinusAlpha -> 0.999, \
                (* sin(beta - alpha) *)
38   lambda6             -> 0, \
                      (* lambda_6 *)
39   lambda7             -> 0, \
                      (* lambda_7 *)
40   TB                  -> 3, \
                      (* tan(beta) = v2/v1 \
   *)
41   m122                -> 200^2, \
                (* m_{12}^2 *)
42   zetau               -> 0, \
                      (* zeta_u *)
43   zetad               -> 0, \
                      (* zeta_d *)
44   zetal               -> 0, \
                      (* zeta_l *)
45   Deltau              -> 0 \
   IdentityMatrix[3],  (* Delta_u *)
46   Deltad              -> 0 \
   IdentityMatrix[3],  (* Delta_d *)
47   Deltal              -> 0 \
   IdentityMatrix[3],  (* Delta_l *)
48   Piu                 -> 0 \
   IdentityMatrix[3],  (* Pi_u *)
49   Pid                 -> 0 \
   IdentityMatrix[3],  (* Pi_d *)
50   Pil                 -> 0 \
   IdentityMatrix[3]   (* Pi_l *)
51   ];
52
53 Print[result];
```

The calculation of a_μ^{BSM} and δa_μ is performed in lines 32–51 with the function `GM2CalcAmuTHDMMassBasis`, which takes the mass basis input parameters as arguments, see Table 3. The result is printed in line 53.

3.7 Running `GM2Calc` from within `Python`

Newly implemented in `GM2Calc` 2.0.0 is the ability to interface with `Python` using the package `cppyy`. An example calculation using the interface is shown in the code snippet below, working in the "mass basis".

```
#!/usr/bin/env python

from __future__ import print_function
from gm2_python_interface import *

cppyy.include(os.path.join
        ("gm2calc","gm2_1loop.hpp"))
cppyy.include(os.path.join
        ("gm2calc","gm2_2loop.hpp"))
cppyy.include(os.path.join
        ("gm2calc","gm2_uncertainty.hpp"))
cppyy.include(os.path.join
        ("gm2calc","gm2_error.hpp"))
cppyy.include(os.path.join
        ("gm2calc","SM.hpp"))
cppyy.include(os.path.join
        ("gm2calc","THDM.hpp"))

cppyy.load_library("libgm2calc")

# Load data types
from cppyy.gbl import Eigen
from cppyy.gbl import gm2calc
from cppyy.gbl.gm2calc import SM
from cppyy.gbl.gm2calc import THDM
from cppyy.gbl.gm2calc import Error

# define THDM parameters in the mass basis
basis = gm2calc.thdm.Mass_basis()
basis.yukawa_type = \
  gm2calc.thdm.Yukawa_type.type_2
basis.mh = 125. \
                                 # light \
  CP-even Higgs mass
basis.mH = 400. \
                                 # heavy \
  CP-even Higgs mass
basis.mA = 420. \
                                 # CP-odd \
  Higgs mass
basis.mHp = 440. \
                                # charged \
  Higgs mass
basis.sin_beta_minus_alpha = 0.999 \
           # sin(beta - alpha)
```

```
36 basis.lambda_6 = 0. \
                                  # lambda_6
37 basis.lambda_7 = 0. \
                                  # lambda_7
38 basis.tan_beta = 3. \
                                  # tan(beta)
39 basis.m122 = 40000. \
                                  # m_{12}^2 in \
     GeV^2
40 basis.zeta_u = 0. \
                                    # zeta_u
41 basis.zeta_d = 0. \
                                    # zeta_d
42 basis.zeta_l = 0. \
                                    # zeta_l
43 basis.Delta_u = \
     Eigen.Matrix3d().setZero() # Delta_u
44 basis.Delta_d = \
     Eigen.Matrix3d().setZero() # Delta_d
45 basis.Delta_l = \
     Eigen.Matrix3d().setZero() # Delta_l
46 basis.Pi_u = Eigen.Matrix3d().setZero() \
        # Pi_u
47 basis.Pi_d = Eigen.Matrix3d().setZero() \
        # Pi_d
48 basis.Pi_l = Eigen.Matrix3d().setZero() \
        # Pi_l
49 # define SM parameters
50 sm = gm2calc.SM()
51 sm.set_alpha_em_mz(1.0/128.94579)   # \
     electromagnetic coupling
52 sm.set_mu(2, 173.34)                # top \
     quark mass
53 sm.set_mu(1, 1.28)                  # \
     charm quark mass
54 sm.set_md(2, 4.18)                  # \
     bottom quark mass
55 sm.set_ml(2, 1.77684)               # tau \
     lepton mass
56 # define options to customize the \
     calculation
57 config = gm2calc.thdm.Config()
58 config.running_couplings = True;    # use \
     running couplings
59
60 try:
61     # setup the THDM
62     model = gm2calc.THDM(basis,sm,config)
63     # calculate a_mu up to (including) \
     the 2-loop level
64     amu = \
     gm2calc.calculate_amu_1loop(model) + \
     gm2calc.calculate_amu_2loop(model)
65     # calculate the uncertainty of the \
     2-loop a_mu
66     delta_amu = \
     gm2calc.calculate_uncertainty_amu_2loop
67            (model)
68     print("amu =",amu,"+-",delta_amu)
69 except gm2calc.Error as e:
70     print(e.what())
```

Note similarity between the above code and the C++ and C interfaces. Line 3 is to make sure that this example which is written using Python 3-style print functions can still work in Python 2. Line 4 imports the interface script gm2_python_interface which loads the cppyy and os packages, as well as the header and library locations.

This interface file is originally in the src subdirectory. After performing

```
1 cmake -DBUILD_SHARED_LIBS=ON ..
```

the interface script will be copied into the subdirectory bin, and it will be filled with the path information for the GM2Calc headers, library, and the Eigen3 path. The interface can be imported from there by other Python scripts, or moved to an appropriate location where the user has their own Python scripts. Lines 6–11 load the relevant header files, and line 13 loads the GM2Calc shared library. In lines 16–20 the necessary namespaces from C++ are loaded into Python. In line 23 the 2HDM Mass_basis object is initialized, while on line 24 the 2HDM is specified to be type II. Lines 25–36 involve setting the values for simple attributes in the basis. Lines 36–42 assign values to the Eigen::Matrix attributes, however since these are meant to be ignored, they are just set to 0. Lines 44–49 initialize an SM object and ensures it has the appropriate parameters. Line 51 initializes the config object, which is used to flag the use of running coupling in the next line. Line 56 initializes a THDM object using the Mass_basis, SM, and Config information. Lines 58–63 prints out the values of a_μ^{BSM} and δa_μ which are calculated using the interface functions calculate_amu_1loop, calculate_amu_2loop, and calculate_uncertainty_amu_2loop. Alternatively an error message will be printed out on line 63 should a problem arise.

Another example of the Python interface is shown below, this time using the "gauge basis":

```
1  #!/usr/bin/env python
2
3  from __future__ import print_function
4  from gm2_python_interface import *
5
6  cppyy.include(os.path.join
7          ("gm2calc","gm2_1loop.hpp"))
8  cppyy.include(os.path.join
9          ("gm2calc","gm2_2loop.hpp"))
10 cppyy.include(os.path.join
11         ("gm2calc","gm2_uncertainty.hpp"))
12 cppyy.include(os.path.join
13         ("gm2calc","gm2_error.hpp"))
14 cppyy.include(os.path.join
15         ("gm2calc","SM.hpp"))
16 cppyy.include(os.path.join
17         ("gm2calc","THDM.hpp"))
18
19 cppyy.load_library("libgm2calc")
20
21 # Load data types
22 from cppyy.gbl import Eigen
23 from cppyy.gbl import gm2calc
24 from cppyy.gbl.gm2calc import SM
25 from cppyy.gbl.gm2calc import THDM
26 from cppyy.gbl.gm2calc import Error
27
28 # define THDM parameters in the mass basis
29 basis = gm2calc.thdm.Gauge_basis()
```

```
30 basis.yukawa_type = \
     gm2calc.thdm.Yukawa_type.type_2
31 # lambda is a reserved keyword, so we have \
     to get creative
32 Matrix7d = Eigen.Matrix('double',7,1)
33 lam = Matrix7d().setZero()
34 lam[0] = 0.7
35 lam[1] = 0.6
36 lam[2] = 0.5
37 lam[3] = 0.4
38 lam[4] = 0.3
39 lam[5] = 0.2
40 lam[6] = 0.1
41 basis.__setattr__('lambda',lam)           \
     # lambda_{1,...,7}
42 basis.tan_beta = 3.                       \
     # tan(beta)
43 basis.m122 = 40000.                       \
     # m_{12}^2 in GeV^2
44 basis.zeta_u = 0.                         \
     # zeta_u
45 basis.zeta_d = 0.                         \
     # zeta_d
46 basis.zeta_l = 0.                         \
     # zeta_l
47 basis.Delta_u = Eigen.Matrix3d().setZero() \
     # Delta_u
48 basis.Delta_d = Eigen.Matrix3d().setZero() \
     # Delta_d
49 basis.Delta_l = Eigen.Matrix3d().setZero() \
     # Delta_l
50 basis.Pi_u = Eigen.Matrix3d().setZero()    \
     # Pi_u
51 basis.Pi_d = Eigen.Matrix3d().setZero()    \
     # Pi_d
52 basis.Pi_l = Eigen.Matrix3d().setZero()    \
     # Pi_l
53 # define SM parameters
54 sm = gm2calc.SM()
55 sm.set_alpha_em_mz(1.0/128.94579)  # \
     electromagnetic coupling
56 sm.set_mu(2, 173.34)               # top \
     quark mass
57 sm.set_mu(1, 1.28)                 # charm \
     quark mass
58 sm.set_md(2, 4.18)                 # \
     bottom quark mass
59 sm.set_ml(2, 1.77684)              # tau \
     lepton mass
60 # define options to customize the \
     calculation
61 config = gm2calc.thdm.Config()
62 config.running_couplings = True;   # use \
     running couplings
63
64 try:
65     # setup the THDM
66     model = gm2calc.THDM(basis,sm,config)
67     # calculate a_mu up to (including) the \
     2-loop level
68     amu = \
     gm2calc.calculate_amu_1loop(model) + \
     gm2calc.calculate_amu_2loop(model)
69     # calculate the uncertainty of the \
     2-loop a_mu
70     delta_amu = \
     gm2calc.calculate_uncertainty_amu_2loop
         (model)
71     print("amu =",amu,"+-",delta_amu)
72 except gm2calc.Error as e:
73     print(e.what())
```

In line 23 we instead initialize a `Gauge_basis` object. To define the attribute `lambda`, we need to circumvent `Python`'s reserved keywords. This is done by defining a 7×1 `Eigen::Matrix` in line 26. This `Matrix` is initialized to 0 before assigned the appropriate entires elementwise on lines 28–34. Then the method `__setattr__` can be used to interface the values to the C++ code. Then the other values can be defined on lines 36–53, and finally the result for a_μ^{BSM} is printed on line 65.

4 Applications

4.1 Parameter scan in the type II and X models

As an application we perform a 2-dimensional parameter scan over m_A and $\tan\beta$ for the type II and type X 2HDM models, similarly to Ref. [85]. However, in contrast to Ref. [85] we include the two-loop bosonic contributions and use the updated value of $a_\mu^{\text{BSM}} = (25.1 \pm 5.9) \times 10^{-10}$ from Eq. (3). The following C++ source code shows the program to perform the scan.

```
#include "gm2calc/gm2_1loop.hpp"
#include "gm2calc/gm2_2loop.hpp"
#include "gm2calc/gm2_error.hpp"
#include "gm2calc/THDM.hpp"

#include <cstdio>
#include <limits>

// Calculates amu in the mA-tan(beta) \
  plane as in Fig.3 from
// arxiv:1409.3199.
double calc_amu(double mA, double tb, \
  gm2calc::thdm::Yukawa_type yukawa_type)
{
   gm2calc::SM sm;
   const double v = sm.get_v();
   const double mh = 126, mH = 200;
   const double lambda_max = \
  3.5449077018110321; // Sqrt[4 Pi]
   const double lambda1 = lambda_max;

   gm2calc::thdm::Mass_basis basis;
   basis.yukawa_type = yukawa_type;
   basis.mh = mh;
   basis.mH = mH;
   basis.mA = mA;
   basis.mHp = mH;
   basis.sin_beta_minus_alpha = 1;
   basis.lambda_6 = 0;
   basis.lambda_7 = 0;
   basis.tan_beta = tb;
   basis.m122 = mH*mH/tb + (mh*mh - \
  lambda1*v*v)/(tb*tb*tb); // Eq.(14)

   double amu = \
  std::numeric_limits<double>::quiet_NaN();

   try {
      gm2calc::THDM model(basis, sm);

```

```
      amu = \
  gm2calc::calculate_amu_1loop(model)
         + \
  gm2calc::calculate_amu_2loop(model);
   } catch (const gm2calc::Error&) {}

   return amu;
}

int main()
{
   const double mA_start = 1, mA_stop = \
  100;
   const double tb_start = 1, tb_stop = \
  100;
   const int N_steps = 198;

   std::printf("%-20s%-20s%-20s%-20s\n",
               "# mA/GeV", "tan(beta)", \
  "amu(II)", "amu(X)");

   for (int i = 0; i <= N_steps; i++) {
      for (int k = 0; k <= N_steps; k++) {
         const double tb = tb_start + \
  i*(tb_stop - tb_start)/N_steps;
         const double mA = mA_start + \
  k*(mA_stop - mA_start)/N_steps;

         const auto type_2 = calc_amu(mA, \
  tb, gm2calc::thdm::Yukawa_type::type_2);
         const auto type_X = calc_amu(mA, \
  tb, gm2calc::thdm::Yukawa_type::type_X);

         std::printf("%-20.10e%-20.10e%
            -20.10e%-20.10e\n",
                     mA, tb, type_2, \
  type_X);
      }
   }

   return 0;
}
```

The function `calc_amu` calculates $a_\mu^{\rm BSM}$ in the 2HDM at the two-loop level for a given value of m_A and $\tan\beta$ and a specified Yukawa type. The remaining 2HDM input parameters in the mass basis are set to $m_h = 126\,\text{GeV}$, $m_H = m_{H^\pm} = 200\,\text{GeV}$, $\sin(\beta-\alpha) = 1$, $\lambda_6 = \lambda_7 = 0$, $m_{12}^2 = m_H^2/\tan\beta + (m_h^2 - \lambda_1 v^2)/\tan^3\beta$ and $\lambda_1 = \sqrt{4\pi}$. In the `main` function the loop over m_A and $\tan\beta$ is performed and $a_\mu^{\rm BSM}$ is calculated for the type II and type X 2HDM and the result is written to the standard output. The 2-dimensional output is shown in Fig. 1 for the two types of the 2HDM.

4.2 Size of fermionic and bosonic contributions

In the following we illustrate the calculation of the two-loop fermionic and bosonic contributions, $a_\mu^{\rm F}$ and $a_\mu^{\rm B}$, separately. For the illustration we perform a scan over m_A for the demo parameter scenario from 2HDMC [113], which is a type II 2HDM scenario where $m_H = 400\,\text{GeV}$, $m_{H^\pm} = 440\,\text{GeV}$, $\tan\beta = 3$, $\sin(\beta-\alpha) = 0.999$, $\lambda_6 = \lambda_7 = 0$ and $m_{12}^2 = (200\,\text{GeV})^2$. The following C source code shows the program to perform the scan.

```
#include "gm2calc/gm2_1loop.h"
#include "gm2calc/gm2_2loop.h"
#include "gm2calc/gm2_error.h"
#include "gm2calc/THDM.h"

#include <stdio.h>

int main()
{
   const double mA_start = 130, mA_stop  = \
  500;
   const int N_steps = 200;

   printf("%-20s%-20s%-20s\n", "# mS/GeV", \
  "amu(F)", "amu(B)");

   for (int i = 0; i <= N_steps; i++) {
      const gm2calc_THDM_mass_basis basis \
  = {
         .yukawa_type = gm2calc_THDM_type_2,
         .mh = 125,
         .mH = 400,
         .mA = mA_start + i*(mA_stop - \
  mA_start)/N_steps,
         .mHp = 440,
         .sin_beta_minus_alpha = 0.999,
         .lambda_6 = 0,
         .lambda_7 = 0,
         .tan_beta = 3,
         .m122 = 40000,
         .zeta_u = 0,
         .zeta_d = 0,
         .zeta_l = 0,
         .Delta_u = { {0,0,0}, {0,0,0}, \
  {0,0,0} },
         .Delta_d = { {0,0,0}, {0,0,0}, \
  {0,0,0} },
         .Delta_l = { {0,0,0}, {0,0,0}, \
  {0,0,0} },
         .Pi_u = { {0,0,0}, {0,0,0}, \
  {0,0,0} },
         .Pi_d = { {0,0,0}, {0,0,0}, \
  {0,0,0} },
         .Pi_l = { {0,0,0}, {0,0,0}, \
  {0,0,0} }
      };

      gm2calc_THDM* model = 0;
      gm2calc_error error = \
  gm2calc_thdm_new_with_mass_basis(&model, \
  &basis, 0, 0);

      if (error == gm2calc_NoError) {
         const double amuF = \
  gm2calc_thdm_calculate_amu_2loop_fermionic
            (model);
         const double amuB = \
  gm2calc_thdm_calculate_amu_2loop_bosonic
            (model);

         printf("%-20.10e%-20.10e%-20.
            10e\n", basis.mA, amuF, amuB);
      } else {
         printf("Error: %s\n", \
  gm2calc_error_str(error));
      }

      gm2calc_thdm_free(model);
   }

   return 0;
}
```

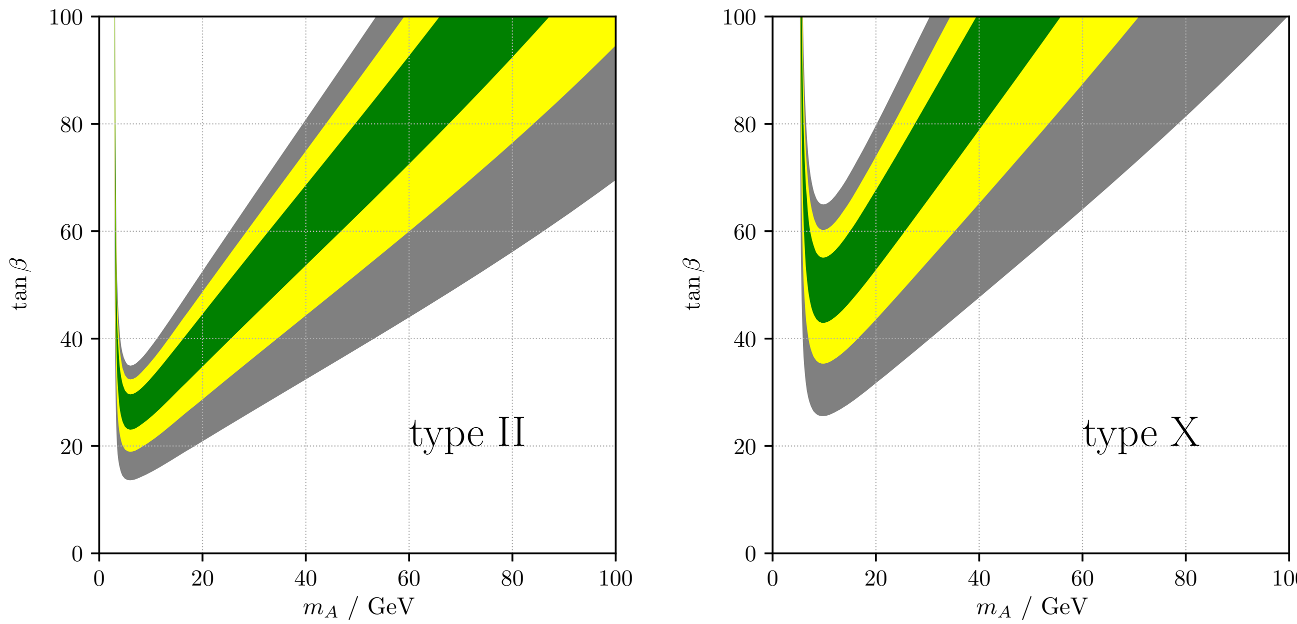

Fig. 1 Two-loop prediction of a_μ^{BSM} in the 2HDM of type II (left) and type X (right) as a function of $\tan\beta$ and m_A with $m_h = 126\,\mathrm{GeV}$, $m_H = m_{H^\pm} = 200\,\mathrm{GeV}$, $\sin(\beta-\alpha) = 1$, $\lambda_6 = \lambda_7 = 0$, $m_{12}^2 = m_H^2/\tan\beta + (m_h^2 - \lambda_1 v^2)/\tan^3\beta$ and $\lambda_1 = \sqrt{4\pi}$. In the green, yellow and gray regions the 2HDM predicts the correct value of $a_\mu^{\mathrm{BSM}} = (25.1 \pm 5.9) \times 10^{-10}$ from Eq. (3) within one, two and three standard deviations, respectively

The SM input parameters and the configuration options are set to their default values by passing 0 as the last two arguments to the function `gm2calc_thdm_new_with_mass_basis` that creates the 2HDM model in line 39. The individual bosonic and fermionic contributions are calculated in lines 42–43 and written to the standard output in line 45.

In the top left panel of Fig. 2 we show the results for the fermionic (red solid line) and bosonic (blue dashed-dotted line) contributions as a function of m_A for this demo scenario from 2HDMC. For the shown parameter space the fermionic contributions decrease, while the bosonic contributions increase for increasing m_A. Furthermore, the bosonic contributions are negative, while the fermionic contributions are positive, which leads to a partial cancellation of the two contributions. However, as is generally the case for the type II 2HDM scenarios that are not already excluded by other constraints, the scenarios we plot here cannot explain the large deviation between the Standard Model prediction and experiment given in Eq. (3).

If instead we consider the FA2HDM scenarios, as in the top right panel of Fig. 2 it is now possible to explain large deviations. Here we fix the following parameters $m_h = 125\,\mathrm{GeV}$, $m_H = 150\,\mathrm{GeV}$, $m_{H^\pm} = 150\,\mathrm{GeV}$, $\sin(\beta-\alpha) = 0.999$, $\lambda_6 = 0$, $\lambda_7 = 0$, $\tan\beta = 2$, $\zeta_u = \zeta_d = -0.1$, $\zeta_l = 50$ based on results used for Fig. 10 of Ref. [103]. It should be noticed that, once the masses for the charged and CP-even scalar are close together and below around 300 GeV, electroweak as well as unitarity and perturbativity constraints can be evaded for arbitrarily low values of m_A [85]. The input parameters here are chosen accordingly. Since $m_A < m_{h_{\mathrm{SM}}}/2$, it is possible for $h \to AA$ decays to occur unless we enforce the coupling $C_{hAA} = 0$.[8] This fixes the value of λ_1 according to Eq. (12) in Ref. [103], which can be set in the mass basis using m_{12}^2 and applying the relations in Eqs. (2.12)–(2.13) in Ref. [102]. This leads to the fitted 2nd-order polynomial relation with a dependence on m_A seen in the source code below.

These scenarios have a very light pseudoscalar mass, but LHC limits are much weaker compared to the type II case and can be evaded for these scenarios. The two-loop fermion contributions rise rapidly as the pseudoscalar mass decreases, dominating over the two-loop bosonic contributions, though the latter are just large enough to have an impact on constraints from a_μ. Note that for higher values of m_A it is possible to get larger bosonic contributions as can be seen in Fig. 10 of Ref. [103]. In the scenarios we plot here the

[8] The coupling C_{hAA} has been discussed in detail in Ref. [103]. Setting $C_{hAA} = 0$ directly corresponds to the choice $\Lambda_6 = 0$, where Λ_6 is a potential parameter in the so-called Higgs basis, and to a specific relation between all potential parameters in the general basis. It has been checked that although non-null values for C_{hAA} can be allowed, they are experimentally strongly constrained. Thus, for simplicity, we have adopted $C_{hAA} = 0$ in our analysis, which automatically guarantees that λ_1 (or equivalently m_{12}^2) will not be chosen in a region excluded by experimental constraints or by unitarity or perturbativity.

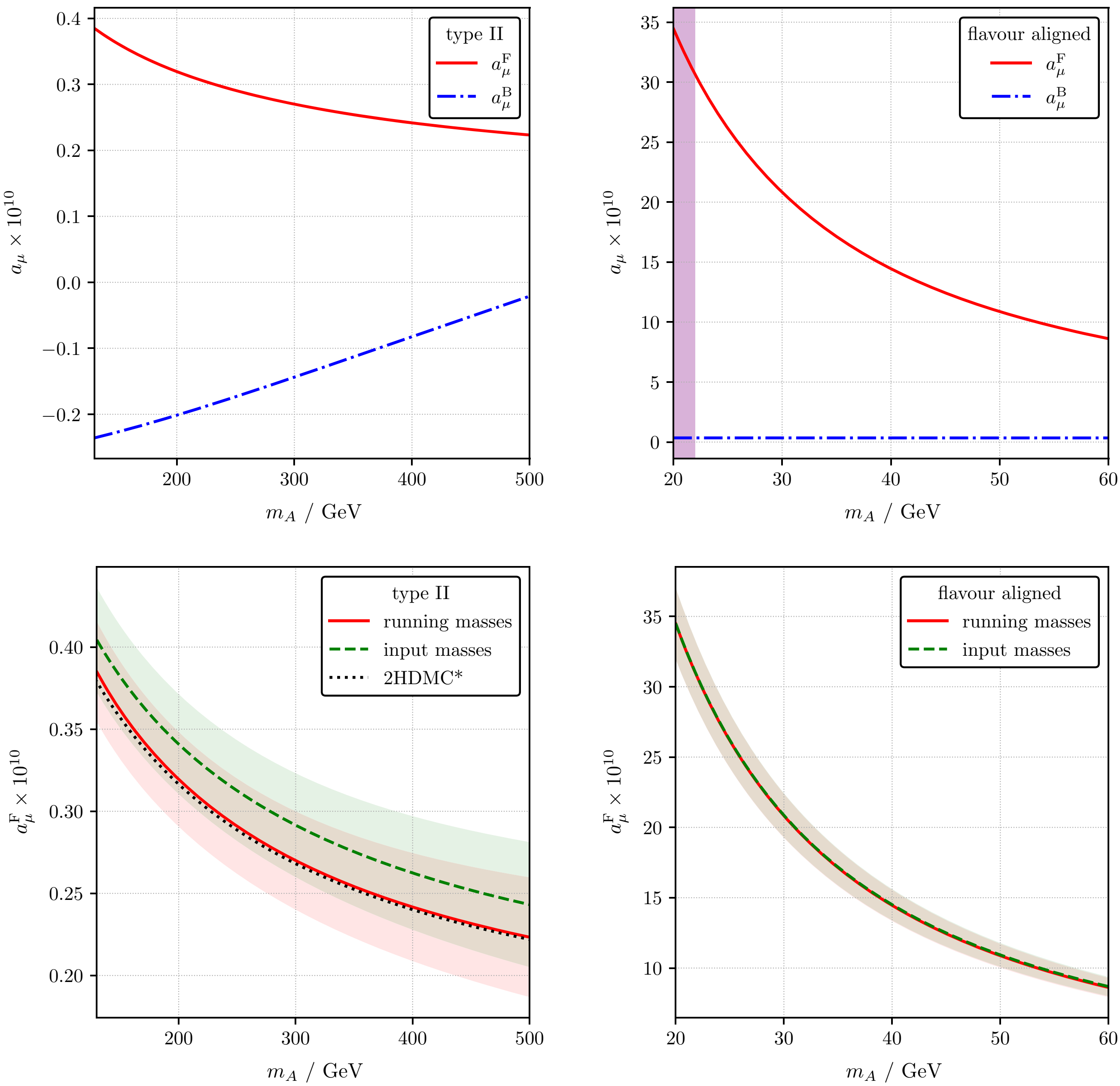

Fig. 2 Different contributions to a_μ^{BSM} in the 2HDM. In the left panels we show scenarios from the type II 2HDM as a function of m_A with $m_H = 400\,\mathrm{GeV}$, $m_{H^\pm} = 440\,\mathrm{GeV}$, $\tan\beta = 3$, $\sin(\beta-\alpha) = 0.999$, $\lambda_6 = \lambda_7 = 0$ and $m_{12}^2 = (200\,\mathrm{GeV})^2$. In the right panels we show FA2HDM scenarios with $m_h = 125\,\mathrm{GeV}$, $m_H = 150\,\mathrm{GeV}$, $m_{H^\pm} = 150\,\mathrm{GeV}$, $\sin(\beta-\alpha) = 0.999$, $\lambda_6 = 0$, $\lambda_7 = 0$, $\tan\beta = 2$, m_{12}^2 is fixed to avoid $h \to AA$ decays using a polynomial equation shown in the related source code, $\zeta_u = \zeta_d = -0.1$, $\zeta_l = 50$ based on scenarios found for Fig. 10 of Ref. [103]. In the top panels we show fermionic (red solid line) and bosonic (blue dashed-dotted line) two-loop contributions separately. The top right panel also shows a purple region over the values of m_A where it is possible to explain Eq. (3). In the bottom panels we compare the fermionic two-loop contributions, when the running 3rd generation fermion masses shown in (73) are used (red solid line) and when the 3rd generation input masses from (72) are used (green dashed line). The red and green bands show the corresponding uncertainties. The bottom left panel also shows two-loop fermionic contributions calculated from `2HDMC` as a black dotted line. *This is not a vanilla `2HDMC` calculation, the SM-Higgs-like two-loop contributions have been removed, and the two-loop charged Higgs Barr–Zee contributions have been added as explained in the text

one-loop contributions, which are not shown in Fig. 2, have a negative effect on the contributions, with a size of approximately one-third of the two-loop fermionic contributions. Thus it can be seen that a_μ^{BSM} can be explained with a very low m_A for the values of m_A in the purple region. The scan for this scenario can be performed with the following C source code:

```
#include "gm2calc/gm2_1loop.h"
#include "gm2calc/gm2_2loop.h"
#include "gm2calc/gm2_error.h"
#include "gm2calc/THDM.h"

#include <stdio.h>
#include <math.h>

int main()
{
   const double mA_start = 20, mA_stop = \
  60;
   const int N_steps = 200;

   printf("%-20s%-20s%-20s%-20s\n", "# \
  mS/GeV", "amu(F)", "amu(B)", "amu(1)");

   for (int i = 0; i <= N_steps; i++) {
      const double mA = mA_start + \
  i*(mA_stop - mA_start)/N_steps;

      const gm2calc_THDM_mass_basis basis \
  = {
         .yukawa_type = \
  gm2calc_THDM_aligned,
         .mh = 125,
         .mH = 150,
         .mA = mA,
         .mHp = 150,
         .sin_beta_minus_alpha = 0.999,
         .lambda_6 = 0,
         .lambda_7 = 0,
         .tan_beta = 2,
         // Polynomial fit following Eq. \
  (2.12) from PRD
         .m122 = 3187.3 + mA*(3.27803 + \
  0.0165557*mA),
         .zeta_u = -0.1,
         .zeta_d = -0.1,
         .zeta_l = 50,
         .Delta_u = { {0,0,0}, {0,0,0}, \
  {0,0,0} },
         .Delta_d = { {0,0,0}, {0,0,0}, \
  {0,0,0} },
         .Delta_l = { {0,0,0}, {0,0,0}, \
  {0,0,0} },
         .Pi_u = { {0,0,0}, {0,0,0}, \
  {0,0,0} },
         .Pi_d = { {0,0,0}, {0,0,0}, \
  {0,0,0} },
         .Pi_l = { {0,0,0}, {0,0,0}, \
  {0,0,0} }
      };

      gm2calc_THDM* model = 0;
      gm2calc_error error = \
  gm2calc_thdm_new_with_mass_basis(&model, \
  &basis, 0, 0);

      if (error == gm2calc_NoError) {
         const double amu1 = \
  gm2calc_thdm_calculate_amu_1loop(model);
         const double amuF = \
  gm2calc_thdm_calculate_amu_2loop_fermionic
            (model);
         const double amuB = \
  gm2calc_thdm_calculate_amu_2loop_bosonic
            (model);

         printf("%-20.10e%-20.10e%-20.10e%
            -20.10e\n", basis.mA, amuF, \
  amuB, amu1);
      } else {
         printf("Error: %s\n", \
  gm2calc_error_str(error));
      }

      gm2calc_thdm_free(model);
   }

   return 0;
}
```

4.3 Running fermion masses

In this subsection we study the effect of using the input vs. running fermion masses in the two-loop fermionic contributions as described in Sect. 2.2.3, and compare the results with `2HDMC`. The following `Mathematica` source code shows a program to perform a scan over m_A using the same type II 2HDM parameter region as in Sect. 4.2.

```
Install["bin/gm2calc.mx"];

CalcAmu[mA_] :=
    {amu2LF, Damu} /. \
  GM2CalcAmuTHDMMassBasis[
        yukawaType          -> 2,
        Mhh                 -> { 125, 400 },
        MAh                 -> mA,
        MHp                 -> 440,
        sinBetaMinusAlpha   -> 0.999,
        lambda6             -> 0,
        lambda7             -> 0,
        TB                  -> 3,
        m122                -> 200^2
    ];

(* mA values in [130,500] GeV *)
mAValues = Subdivide[130, 500, 200];

(* calculation w/o running couplings *)
GM2CalcSetFlags[runningCouplings -> False];
noRunning = CalcAmu /@ mAValues;

(* calculation w/ running couplings *)
GM2CalcSetFlags[runningCouplings -> True];
withRunning = CalcAmu /@ mAValues;

data = { mAValues,
         noRunning[[All,1]], \
  noRunning[[All,2]],
         withRunning[[All,1]], \
  withRunning[[All,2]] };

Export["running.txt", N @ Transpose @ \
  data, "Table"];
```

The function CalcAmu calculates the two-loop fermionic contribution a_μ^{F} and the uncertainty δa_μ for a given value of m_A and the mass basis input parameters defined above. In line 20 the usage of running fermion masses is disabled and the calculation is performed in the subsequent line. Similarly, in line 24 the usage of running fermion masses is enabled and the calculation is performed in the subsequent line. The results are collected in the variable data and are exported to a file in line 31. We also used a very similar script to do the same calculations for the FA2HDM scenarios discussed in Sect. 4.2.

The effect of using running fermion masses in the two-loop fermionic contributions is shown in Fig. 2 for the type II (bottom left panel) and flavour aligned (bottom right panel) scenarios matching those described in the previous section. The red solid line shows the value of a_μ^{F} when the running masses (73) are used, i.e. the 3rd generation fermion masses are run to the scale of the Higgs boson in the two-loop fermionic Barr-Zee Feynman diagrams. Note that although the vertical axes are slightly different, the red lines shown in the bottom panels are identical to the red lines from the corresponding panels immediately above them, which were discussed in the previous section. The green dashed lines show the value of a_μ^{F} when input fermion masses listed in (72) are used. In both scenarios that we look at the value of a_μ^{F} is smaller when running masses are used, though the difference is only distinguishable for the type II case where the size of the contributions is much smaller. The reason for this is that due to the negative fermion mass β functions the running masses are numerically smaller than the corresponding input masses in the shown scenarios, which leads to a systematic reduction of the fermionic two-loop contributions.

In addition to the red solid and green dashed lines from GM2Calc, as the scenario in question is a benchmark point for 2HDMC [113], we show in the bottom left panel of Fig. 2 the corresponding result obtained with 2HDMC 1.8.0 as black dotted line. Note that at the two-loop level 2HDMC includes only fermionic contributions to a_μ^{BSM}. Furthermore, 2HDMC does not subtract the contributions from the SM Higgs boson and does not include the two-loop contributions from the charged Higgs boson. Therefore to obtain this black dotted line we have thus subtracted the two-loop SM Higgs contributions from the 2HDMC result and added the two-loop contributions from the charged Higgs boson. Since 2HDMC inserts running fermion masses into the fermionic contributions, the black dotted line can be compared to the red solid line in the figure. There is a small deviation between these two lines, which originates from the inclusion of fermionic Barr-Zee diagrams with an internal Z boson in GM2Calc, which are not included in 2HDMC.

In the bottom panels of Fig. 2 we also show the uncertainties calculated with (74) as lighter shaded regions of the corresponding color about the red and green lines. In the bottom left panel the red and green lines both lie within the uncertainty estimate for the alternative prediction (shaded green and shaded red regions respectively) for all values of m_A plotted. This is also true in the bottom right panel though there is no visible distinction between the red and green lines or their uncertainties here. Since the difference between the lines is of higher order, this indicates that our uncertainty estimate is working as expected and accounts for the expected higher order corrections.

5 Summary

We have presented version 2 of GM2Calc, with its new capability to calculate the BSM contributions to the anomalous magnetic moment of the muon in the 2HDM. The contributions include all the one-loop diagrams, two-loop fermionic Bar-Zee diagrams, as well as the bosonic two-loop contributions. The new version of GM2Calc provides the calculation of the 2HDM contributions with a precision of up to $\mathcal{O}(m_\mu^4)$ at one-loop and $\mathcal{O}(m_\mu^2)$ at two-loop level along with an estimate of uncertainty of the evaluation. GM2Calc performs this state of the art precision calculation at high speed, with execution times that can be as short as $\mathcal{O}(0.05\,\mathrm{ms})$ per point, allowing for rapid sampling of the parameter space. GM2Calc is easy to configure and run. The user can select well-known types of the 2HDM, specifically type I, II, X, Y as well as the flavour-aligned version (FA2HDM), or the fully general 2HDM. For the latter the user can specify the inputs as deviations away from the flavour alignment of the FA2HDM (or from type I, II, X, and Y) or by directly specifying the more fundamental Yukawa matrices, Π_f defined in Eq. (27). The user can also decide whether they will give inputs in the gauge basis using $\lambda_{1,\ldots,7}$ or the mass basis using $m_{h,H,A,H^\pm}$, $\lambda_{6,7}$, and $\sin(\beta-\alpha)$. The input parameters and settings can be specified in an SLHA-like input file, mirroring the original MSSM version. Additionally, GM2Calc can be interfaced to other programs using C++, C, Mathematica, or Python, the latter being a new interface developed for GM2Calc 2.

For each of these interfaces we presented simple and easy to follow usage examples in Sect. 3, that are straightforward to adapt. In Sect. 4 we have also presented some applications and results, demonstrating different features of the code. In each of these we show the source code in the manual and also provide them as supplementary files. GM2Calc is actively developed on GitHub and users with any questions may contact the authors through our GitHub page or directly by email.

Acknowledgements We would like to thank the other authors of version 1 of GM2Calc, M. Bach, H. G. Fargnoli, C. Gnendiger, R. Greifenhagen, J. Park, and S. Paßehr. We also thank T Gonzalo and C. S. Fonseca for their assistance with work dealing with two-loop contributions to the anomalous magnetic moment of the muon. The research placement of D.J. for this work was supported by the Australian Government Research Training Program (RTP) Scholarship and the Deutscher Akademischer Austauschdienst (DAAD) One-Year Research Grant. The work of P.A. was supported by the Australian Research Council Future Fellowship grant FT160100274. The work of P.A. and C.B. was also supported with the Australian Research Council Discovery Project grant DP180102209. This project was undertaken with the assistance of resources and services from the National Computational Infrastructure, which is supported by the Australian Government. We thank Astronomy Australia Limited for financial support of computing resources.

Data Availability Statement This manuscript has no associated data or the data will not be deposited. [Author's comment: The data used to create Figures 1 and 2 can be reproduced with GM2Calc 2.0.0 using the source code examples in the paper.]

Funded by SCOAP[3].

References

1. Muon $g-2$ Collaboration collaboration, B. Abi et al., Measurement of the positive muon anomalous magnetic moment to 0.46 ppm. Phys. Rev. Lett. **126**, 141801 (2021). https://doi.org/10.1103/PhysRevLett.126.141801
2. Particle Data Group collaboration, M. Tanabashi et al., Review of particle physics. Phys. Rev. D **98**, 030001 (2018). https://doi.org/10.1103/PhysRevD.98.030001
3. T. Aoyama et al., The anomalous magnetic moment of the muon in the standard model. Phys. Rep. **887**, 1–166 (2020). arXiv:2006.04822
4. T. Aoyama, M. Hayakawa, T. Kinoshita, M. Nio, Complete tenth-order QED contribution to the Muon $g-2$. Phys. Rev. Lett. **109**, 111808 (2012). https://doi.org/10.1103/PhysRevLett.109.111808 arXiv:1205.5370
5. T. Aoyama, T. Kinoshita, M. Nio, Theory of the anomalous magnetic moment of the electron. Atoms **7**, 28 (2019). https://doi.org/10.3390/atoms7010028
6. A. Czarnecki, W.J. Marciano, A. Vainshtein, Refinements in electroweak contributions to the muon anomalous magnetic moment. Phys. Rev. D **67**, 073006 (2003). https://doi.org/10.1103/PhysRevD.67.073006 arXiv:hep-ph/0212229
7. C. Gnendiger, D. Stöckinger, H. Stöckinger-Kim, The electroweak contributions to $(g-2)_\mu$ after the Higgs boson mass measurement. Phys. Rev. D **88**, 053005 (2013). https://doi.org/10.1103/PhysRevD.88.053005 arXiv:1306.5546
8. M. Davier, A. Hoecker, B. Malaescu, Z. Zhang, Reevaluation of the hadronic vacuum polarisation contributions to the Standard Model predictions of the muon $g-2$ and $\alpha(m_Z^2)$ using newest hadronic cross-section data. Eur. Phys. J. C **77**, 827 (2017). https://doi.org/10.1140/epjc/s10052-017-5161-6 arXiv:1706.09436
9. A. Keshavarzi, D. Nomura, T. Teubner, Muon $g-2$ and $\alpha(M_Z^2)$: a new data-based analysis. Phys. Rev. D **97**, 114025 (2018). https://doi.org/10.1103/PhysRevD.97.114025 arXiv:1802.02995
10. G. Colangelo, M. Hoferichter, P. Stoffer, Two-pion contribution to hadronic vacuum polarization. JHEP **02**, 006 (2019). https://doi.org/10.1007/JHEP02(2019)006 arXiv:1810.00007
11. M. Hoferichter, B.-L. Hoid, B. Kubis, Three-pion contribution to hadronic vacuum polarization. JHEP **08**, 137 (2019). https://doi.org/10.1007/JHEP08(2019)137 arXiv:1907.01556
12. M. Davier, A. Hoecker, B. Malaescu, Z. Zhang, A new evaluation of the hadronic vacuum polarisation contributions to the muon anomalous magnetic moment and to $\boldsymbol{\alpha}(\mathbf{m}_\mathbf{Z}^2)$. Eur. Phys. J. C **80**, 241 (2020). https://doi.org/10.1140/epjc/s10052-020-7792-2 arXiv:1908.00921
13. A. Keshavarzi, D. Nomura, T. Teubner, The $g-2$ of charged leptons, $\alpha(M_Z^2)$ and the hyperfine splitting of muonium. Phys. Rev. D **101**, 014029 (2020). https://doi.org/10.1103/PhysRevD.101.014029 arXiv:1911.00367
14. A. Kurz, T. Liu, P. Marquard, M. Steinhauser, Hadronic contribution to the muon anomalous magnetic moment to next-to-next-to-leading order. Phys. Lett. B **734**, 144–147 (2014). https://doi.org/10.1016/j.physletb.2014.05.043 arXiv:1403.6400
15. K. Melnikov, A. Vainshtein, Hadronic light-by-light scattering contribution to the muon anomalous magnetic moment revisited. Phys. Rev. D **70**, 113006 (2004). https://doi.org/10.1103/PhysRevD.70.113006 arXiv:hep-ph/0312226
16. P. Masjuan, P. Sánchez-Puertas, Pseudoscalar-pole contribution to the $(g_\mu-2)$: a rational approach. Phys. Rev. D **95**, 054026 (2017). https://doi.org/10.1103/PhysRevD.95.054026 arXiv:1701.05829
17. G. Colangelo, M. Hoferichter, M. Procura, P. Stoffer, Dispersion relation for hadronic light-by-light scattering: two-pion contributions. JHEP **04**, 161 (2017). https://doi.org/10.1007/JHEP04(2017)161 arXiv:1702.07347
18. M. Hoferichter, B.-L. Hoid, B. Kubis, S. Leupold, S.P. Schneider, Dispersion relation for hadronic light-by-light scattering: pion pole. JHEP **10**, 141 (2018). https://doi.org/10.1007/JHEP10(2018)141 arXiv:1808.04823
19. A. Gérardin, H.B. Meyer, A. Nyffeler, Lattice calculation of the pion transition form factor with $N_f=2+1$ Wilson quarks. Phys. Rev. D **100**, 034520 (2019). https://doi.org/10.1103/PhysRevD.100.034520 arXiv:1903.09471
20. J. Bijnens, N. Hermansson-Truedsson, A. Rodríguez-Sánchez, Short-distance constraints for the HLbL contribution to the muon anomalous magnetic moment. Phys. Lett. B **798**, 134994 (2019). https://doi.org/10.1016/j.physletb.2019.134994 arXiv:1908.03331
21. G. Colangelo, F. Hagelstein, M. Hoferichter, L. Laub, P. Stoffer, Longitudinal short-distance constraints for the hadronic light-by-light contribution to $(g-2)_\mu$ with large-N_c Regge models. JHEP **03**, 101 (2020). https://doi.org/10.1007/JHEP03(2020)101 arXiv:1910.13432
22. V. Pauk, M. Vanderhaeghen, Single meson contributions to the muon's anomalous magnetic moment. Eur. Phys. J. C **74**, 3008 (2014). https://doi.org/10.1140/epjc/s10052-014-3008-y arXiv:1401.0832
23. I. Danilkin, M. Vanderhaeghen, Light-by-light scattering sum rules in light of new data. Phys. Rev. D **95**, 014019 (2017). https://doi.org/10.1103/PhysRevD.95.014019 arXiv:1611.04646
24. F. Jegerlehner, The anomalous magnetic moment of the muon. Springer Tracts Mod. Phys. **274**, 1–693 (2017). https://doi.org/10.1007/978-3-319-63577-4
25. M. Knecht, S. Narison, A. Rabemananjara, D. Rabetiarivony, Scalar meson contributions to a_μ from hadronic light-by-light scattering. Phys. Lett. B **787**, 111–123 (2018). https://doi.org/10.1016/j.physletb.2018.10.048 arXiv:1808.03848

26. G. Eichmann, C.S. Fischer, R. Williams, Kaon-box contribution to the anomalous magnetic moment of the muon. Phys. Rev. D **101**, 054015 (2020). https://doi.org/10.1103/PhysRevD.101.054015 arXiv:1910.06795
27. P. Roig, P. Sánchez-Puertas, Axial-vector exchange contribution to the hadronic light-by-light piece of the muon anomalous magnetic moment. Phys. Rev. D **101**, 074019 (2020). https://doi.org/10.1103/PhysRevD.101.074019 arXiv:1910.02881
28. T. Blum, N. Christ, M. Hayakawa, T. Izubuchi, L. Jin, C. Jung et al., The hadronic light-by-light scattering contribution to the muon anomalous magnetic moment from lattice QCD. Phys. Rev. Lett. **124**, 132002 (2020). https://doi.org/10.1103/PhysRevLett.124.132002 arXiv:1911.08123
29. G. Colangelo, M. Hoferichter, A. Nyffeler, M. Passera, P. Stoffer, Remarks on higher-order hadronic corrections to the muon $g-2$. Phys. Lett. B **735**, 90–91 (2014). https://doi.org/10.1016/j.physletb.2014.06.012 arXiv:1403.7512
30. Fermilab Lattice, LATTICE-HPQCD, MILC collaboration, B. Chakraborty et al., Strong-isospin-breaking correction to the muon anomalous magnetic moment from lattice QCD at the physical point. Phys. Rev. Lett. **120**, 152001 (2018). https://doi.org/10.1103/PhysRevLett.120.152001. arXiv:1710.11212
31. Budapest-Marseille-Wuppertal collaboration, S. Borsanyi et al., Hadronic vacuum polarization contribution to the anomalous magnetic moments of leptons from first principles. Phys. Rev. Lett. **121**, 022002 (2018). https://doi.org/10.1103/PhysRevLett.121.022002. arXiv:1711.04980
32. RBC, UKQCD collaboration, T. Blum, P. A. Boyle, V. Gülpers, T. Izubuchi, L. Jin, C. Jung et al., Calculation of the hadronic vacuum polarization contribution to the muon anomalous magnetic moment. Phys. Rev. Lett. **121**, 022003 (2018). https://doi.org/10.1103/PhysRevLett.121.022003. arXiv:1801.07224
33. D. Giusti, V. Lubicz, G. Martinelli, F. Sanfilippo, S. Simula, Electromagnetic and strong isospin-breaking corrections to the muon $g-2$ from Lattice QCD + QED. Phys. Rev. D **99**, 114502 (2019). https://doi.org/10.1103/PhysRevD.99.114502 arXiv:1901.10462
34. PACS collaboration, E. Shintani, Y. Kuramashi, Hadronic vacuum polarization contribution to the muon $g-2$ with 2+1 flavor lattice QCD on a larger than (10 fm)^4 lattice at the physical point. Phys. Rev. D **100**, 034517 (2019). https://doi.org/10.1103/PhysRevD.100.034517. arXiv:1902.00885
35. Fermilab Lattice, LATTICE-HPQCD, MILC collaboration, C.T.H. Davies et al., Hadronic-vacuum-polarization contribution to the muon's anomalous magnetic moment from four-flavor lattice QCD. Phys. Rev. D **101**, 034512 (2020). https://doi.org/10.1103/PhysRevD.101.034512. arXiv:1902.04223
36. A. Gérardin, M. Cè, G. von Hippel, B. Hörz, H.B. Meyer, D. Mohler et al., The leading hadronic contribution to $(g-2)_\mu$ from lattice QCD with $N_f = 2+1$ flavours of O(a) improved Wilson quarks. Phys. Rev. D **100**, 014510 (2019). https://doi.org/10.1103/PhysRevD.100.014510 arXiv:1904.03120
37. C. Aubin, T. Blum, C. Tu, M. Golterman, C. Jung, S. Peris, Light quark vacuum polarization at the physical point and contribution to the muon $g-2$. Phys. Rev. D **101**, 014503 (2020). https://doi.org/10.1103/PhysRevD.101.014503 arXiv:1905.09307
38. D. Giusti, S. Simula, Lepton anomalous magnetic moments in Lattice QCD+QED. PoS **LATTICE2019**, 104 (2019). https://doi.org/10.22323/1.363.0104 arXiv:1910.03874
39. S. Borsanyi et al., Leading hadronic contribution to the muon 2 magnetic moment from lattice QCD. arXiv:2002.12347
40. C. Lehner, A.S. Meyer, Consistency of hadronic vacuum polarization between lattice QCD and the R-ratio. Phys. Rev. D **101**, 074515 (2020). https://doi.org/10.1103/PhysRevD.101.074515 arXiv:2003.04177
41. G. Colangelo, M. Hoferichter, P. Stoffer, Constraints on the two-pion contribution to hadronic vacuum polarization. Phys. Lett. B **814**, 136073 (2021). https://doi.org/10.1016/j.physletb.2021.136073 arXiv:2010.07943
42. G.C. Branco, P.M. Ferreira, L. Lavoura, M.N. Rebelo, M. Sher, J.P. Silva, Theory and phenomenology of two-Higgs-doublet models. Phys. Rep. **516**, 1–102 (2012). https://doi.org/10.1016/j.physrep.2012.02.002 arXiv:1106.0034
43. J.F. Gunion, H.E. Haber, G.L. Kane, S. Dawson, The Higgs Hunter's Guide, vol. 80 (2000)
44. ATLAS collaboration, G. Aad et al., Observation of a new particle in the search for the Standard Model Higgs boson with the ATLAS detector at the LHC. Phys. Lett. B **716**, 1–29 (2012). https://doi.org/10.1016/j.physletb.2012.08.020. arXiv:1207.7214
45. CMS collaboration, S. Chatrchyan et al., Observation of a new boson at a mass of 125 GeV with the CMS experiment at the LHC. Phys. Lett. B **716**, 30–61 (2012). https://doi.org/10.1016/j.physletb.2012.08.021. arXiv:1207.7235
46. H.E. Haber, O. Stål, New LHC benchmarks for the $mathcal CP$-conserving two-Higgs-doublet model. Eur. Phys. J. C **75**, 491 (2015). https://doi.org/10.1140/epjc/s10052-015-3697-x arXiv:1507.04281
47. J. Baglio, O. Eberhardt, U. Nierste, M. Wiebusch, Benchmarks for Higgs pair production and heavy Higgs boson searches in the Two-Higgs-Doublet Model of Type II. Phys. Rev. D **90**, 015008 (2014). https://doi.org/10.1103/PhysRevD.90.015008 arXiv:1403.1264
48. O. Eberhardt, U. Nierste, M. Wiebusch, Status of the two-Higgs-doublet model of type II. JHEP **07**, 118 (2013). https://doi.org/10.1007/JHEP07(2013)118 arXiv:1305.1649
49. D. Chowdhury, O. Eberhardt, Global fits of the two-loop renormalized Two-Higgs-Doublet model with soft Z_2 breaking. JHEP **11**, 052 (2015). https://doi.org/10.1007/JHEP11(2015)052 arXiv:1503.08216
50. D. Chowdhury, O. Eberhardt, Update of global two-Higgs-doublet model fits. JHEP **05**, 161 (2018). https://doi.org/10.1007/JHEP05(2018)161 arXiv:1711.02095
51. M. Misiak, M. Steinhauser, Weak radiative decays of the B meson and bounds on $M_{H^\pm}$ in the Two-Higgs-Doublet Model. Eur. Phys. J. C **77**, 201 (2017). https://doi.org/10.1140/epjc/s10052-017-4776-y arXiv:1702.04571
52. Q.-Y. Hu, X.-Q. Li, Y.-D. Yang, $B^0 \to K^{*0}\mu^+\mu^-$ decay in the aligned two-Higgs-doublet model. Eur. Phys. J. C **77**, 190 (2017). https://doi.org/10.1140/epjc/s10052-017-4748-2 arXiv:1612.08867
53. X.-Q. Li, J. Lu, A. Pich, $B^0_{s,d} \to \ell^+\ell^-$ decays in the aligned two-Higgs-doublet model. JHEP **06**, 022 (2014). https://doi.org/10.1007/JHEP06(2014)022 arXiv:1404.5865
54. T. Enomoto, R. Watanabe, Flavor constraints on the Two Higgs Doublet Models of Z_2 symmetric and aligned types. JHEP **05**, 002 (2016). https://doi.org/10.1007/JHEP05(2016)002 arXiv:1511.05066
55. P. Arnan, D. Bečirević, F. Mescia, O. Sumensari, Two Higgs doublet models and $b \to s$ exclusive decays. Eur. Phys. J. C **77**, 796 (2017). https://doi.org/10.1140/epjc/s10052-017-5370-z arXiv:1703.03426
56. A. Barroso, P.M. Ferreira, I.P. Ivanov, R. Santos, Metastability bounds on the two Higgs doublet model. JHEP **06**, 045 (2013). https://doi.org/10.1007/JHEP06(2013)045 arXiv:1303.5098
57. P.S. Bhupal Dev, A. Pilaftsis, Maximally symmetric two Higgs doublet model with natural standard model alignment. JHEP **12**, 024 (2014). https://doi.org/10.1007/JHEP12(2014)024 arXiv:1408.3405
58. S. Kanemura, K. Yagyu, Unitarity bound in the most general two Higgs doublet model. Phys. Lett. B **751**, 289–296 (2015). https://doi.org/10.1016/j.physletb.2015.10.047 arXiv:1509.06060
59. P. Draper, A. Ekstedt, H.E. Haber, A natural mechanism for approximate Higgs alignment in the 2HDM. JHEP **05**, 235 (2021). https://doi.org/10.1007/JHEP05(2021)235 arXiv:2011.13159

60. S. Gori, H.E. Haber, E. Santos, High scale flavor alignment in two-Higgs doublet models and its phenomenology. JHEP **06**, 110 (2017). https://doi.org/10.1007/JHEP06(2017)110 arXiv:1703.05873
61. P. Basler, M. Krause, M. Muhlleitner, J. Wittbrodt, A. Wlotzka, Strong first order electroweak phase transition in the CP-conserving 2HDM revisited. JHEP **02**, 121 (2017). https://doi.org/10.1007/JHEP02(2017)121 arXiv:1612.04086
62. P. Basler, M. Mühlleitner, J. Wittbrodt, The CP-violating 2HDM in light of a strong first order electroweak phase transition and implications for Higgs pair production. JHEP **03**, 061 (2018). https://doi.org/10.1007/JHEP03(2018)061 arXiv:1711.04097
63. P. Basler, M. Mühlleitner, J. Müller, Electroweak phase transition in non-minimal Higgs sectors. JHEP **05**, 016 (2020). https://doi.org/10.1007/JHEP05(2020)016 arXiv:1912.10477
64. K. Kainulainen, V. Keus, L. Niemi, K. Rummukainen, T.V.I. Tenkanen, V. Vaskonen, On the validity of perturbative studies of the electroweak phase transition in the Two Higgs Doublet model. JHEP **06**, 075 (2019). https://doi.org/10.1007/JHEP06(2019)075 arXiv:1904.01329
65. P. Basler, M. Mühlleitner, J. Müller, Electroweak baryogenesis in the CP-violating two-Higgs doublet model. arXiv:2108.03580
66. M. Krause, R. Lorenz, M. Muhlleitner, R. Santos, H. Ziesche, Gauge-independent renormalization of the 2-Higgs-doublet model. JHEP **09**, 143 (2016). https://doi.org/10.1007/JHEP09(2016)143 arXiv:1605.04853
67. M. Krause, M. Muhlleitner, R. Santos, H. Ziesche, Higgs-to-Higgs boson decays in a 2HDM at next-to-leading order. Phys. Rev. D **95**, 075019 (2017). https://doi.org/10.1103/PhysRevD.95.075019 arXiv:1609.04185
68. L. Altenkamp, S. Dittmaier, H. Rzehak, Precision calculations for $h \to WW/ZZ \to 4$ fermions in the two-Higgs-Doublet Model with Prophecy4f. JHEP **03**, 110 (2018). https://doi.org/10.1007/JHEP03(2018)110 arXiv:1710.07598
69. L. Altenkamp, S. Dittmaier, H. Rzehak, Renormalization schemes for the Two-Higgs-Doublet Model and applications to h $\to$ WW/ZZ $\to$ 4 fermions. JHEP **09**, 134 (2017). https://doi.org/10.1007/JHEP09(2017)134 arXiv:1704.02645
70. L. Altenkamp, M. Boggia, S. Dittmaier, H. Rzehak, Electroweak corrections in the two-Higgs-doublet model and singlet extension of the standard model. PoS **LL2018**, 011 (2018). https://doi.org/10.22323/1.303.0011 arXiv:1807.05876
71. A. Denner, S. Dittmaier, J.-N. Lang, Renormalization of mixing angles. JHEP **11**, 104 (2018). https://doi.org/10.1007/JHEP11(2018)104 arXiv:1808.03466
72. S. Kanemura, M. Kikuchi, K. Mawatari, K. Sakurai, K. Yagyu, Loop effects on the Higgs decay widths in extended Higgs models. Phys. Lett. B **783**, 140–149 (2018). https://doi.org/10.1016/j.physletb.2018.06.035 arXiv:1803.01456
73. M. Krause, M. Mühlleitner, Impact of electroweak corrections on neutral Higgs boson decays in extended Higgs sectors. JHEP **04**, 083 (2020). https://doi.org/10.1007/JHEP04(2020)083 arXiv:1912.03948
74. M. Aiko, S. Kanemura, K. Sakurai, Radiative corrections to decays of charged Higgs bosons in two Higgs doublet models. arXiv:2108.11868
75. P. Athron, C. Balázs, D.H.J. Jacob, W. Kotlarski, D. Stöckinger, H. Stöckinger-Kim, New physics explanations of a_μ in light of the FNAL muon g-2 measurement. J. High Energy Phys. **2021**, 80 (2021). https://doi.org/10.1007/JHEP09(2021)080 arXiv:2104.03691
76. V.D. Barger, J.L. Hewett, R.J.N. Phillips, New constraints on the charged Higgs sector in two Higgs doublet models. Phys. Rev. D **41**, 3421–3441 (1990). https://doi.org/10.1103/PhysRevD.41.3421
77. H.E. Haber, G.L. Kane, T. Sterling, The Fermion mass scale and possible effects of Higgs bosons on experimental observables. Nucl. Phys. B **161**, 493–532 (1979). https://doi.org/10.1016/0550-3213(79)90225-6
78. L.J. Hall, M.B. Wise, Flavor changing Higgs-boson couplings. Nucl. Phys. B **187**, 397–408 (1981). https://doi.org/10.1016/0550-3213(81)90469-7
79. R.M. Barnett, G. Senjanovic, L. Wolfenstein, D. Wyler, Implications of a light Higgs scalar. Phys. Lett. B **136**, 191–195 (1984). https://doi.org/10.1016/0370-2693(84)91179-1
80. R.M. Barnett, G. Senjanovic, D. Wyler, Tracking down Higgs scalars with enhanced couplings. Phys. Rev. D **30**, 1529 (1984). https://doi.org/10.1016/0370-2693(84)91179-1
81. V. Barger, H.E. Logan, G. Shaughnessy, Identifying extended Higgs models at the LHC. Phys. Rev. D **79**, 115018 (2009). https://doi.org/10.1103/PhysRevD.79.115018 arXiv:0902.0170
82. H.E. Logan, D. MacLennan, Charged Higgs phenomenology in the flipped two Higgs doublet model. Phys. Rev. D **81**, 075016 (2010). https://doi.org/10.1103/PhysRevD.81.075016 arXiv:1002.4916
83. A. Pich, P. Tuzon, Yukawa alignment in the two-Higgs-doublet model. Phys. Rev. D **80**, 091702 (2009). https://doi.org/10.1103/PhysRevD.80.091702 arXiv:0908.1554
84. P. Tuzon, A. Pich, The aligned two-Higgs doublet model. Acta Phys. Polon. Supp. **3**, 215–220 (2010). arXiv:1001.0293
85. A. Broggio, E.J. Chun, M. Passera, K.M. Patel, S.K. Vempati, Limiting two-Higgs-doublet models. JHEP **11**, 058 (2014). https://doi.org/10.1007/JHEP11(2014)058 arXiv:1409.3199
86. L. Wang, X.-F. Han, A light pseudoscalar of 2HDM confronted with muon g-2 and experimental constraints. JHEP **05**, 039 (2015). https://doi.org/10.1007/JHEP05(2015)039 arXiv:1412.4874
87. T. Abe, R. Sato, K. Yagyu, Lepton-specific two Higgs doublet model as a solution of muon g - 2 anomaly. JHEP **07**, 064 (2015). https://doi.org/10.1007/JHEP07(2015)064 arXiv:1504.07059
88. E.J. Chun, The muon g−2 in two-Higgs-doublet models. EPJ Web Conf. **118**, 01006 (2016). https://doi.org/10.1051/epjconf/201611801006 arXiv:1511.05225
89. E.J. Chun, Z. Kang, M. Takeuchi, Y.-L.S. Tsai, LHC τ-rich tests of lepton-specific 2HDM for (g - 2)$_\mu$. JHEP **11**, 099 (2015). https://doi.org/10.1007/JHEP11(2015)099 [arxiv:1507.08067]
90. E.J. Chun, J. Kim, Leptonic precision test of leptophilic two-Higgs-doublet model. JHEP **07**, 110 (2016). https://doi.org/10.1007/JHEP07(2016)110 arXiv:1605.06298
91. L. Wang, J.M. Yang, M. Zhang, Y. Zhang, Revisiting lepton-specific 2HDM in light of muon $g-2$ anomaly. Phys. Lett. B **788**, 519–529 (2019). https://doi.org/10.1016/j.physletb.2018.11.045 arXiv:1809.05857
92. E.J. Chun, J. Kim, T. Mondal, Electron EDM and Muon anomalous magnetic moment in Two-Higgs-Doublet Models. JHEP **12**, 068 (2019). https://doi.org/10.1007/JHEP12(2019)068 arXiv:1906.00612
93. E.J. Chun, T. Mondal, Searching for a light Higgs boson via the Yukawa process at lepton colliders. Phys. Lett. B **802**, 135190 (2020). https://doi.org/10.1016/j.physletb.2019.135190 arXiv:1909.09515
94. W.-Y. Keung, D. Marfatia, P.-Y. Tseng, Axion-like particles, two-Higgs-doublet models, leptoquarks, and the electron and Muon g-2. LHEP **2021**, 209 (2021). https://doi.org/10.31526/lhep.2021.209 arXiv:2104.03341
95. P.M. Ferreira, B.L. Gonçalves, F.R. Joaquim, M. Sher, (g-2)μ in the 2HDM and slightly beyond: an updated view. Phys. Rev. D **104**, 053008 (2021). https://doi.org/10.1103/PhysRevD.104.053008 arXiv:2104.03367
96. X.-F. Han, T. Li, H.-X. Wang, L. Wang, Y. Zhang, Lepton-specific inert two-Higgs-doublet model confronted with the new results for

muon and electron g-2 anomalies and multi-lepton searches at the LHC. arXiv:2104.03227
97. J.C. Eung, T. Mondal, Leptophilic bosons and muon g-2 at lepton colliders. JHEP **07**, 044 (2021). https://doi.org/10.1007/JHEP07(2021)044 arXiv:2104.03701
98. A. Jueid, J. Kim, S. Lee, J. Song, Type-X two Higgs doublet model in light of the muon $\mathbf{g-2}$: confronting Higgs and collider data. arXiv:2104.10175
99. A. Dey, J. Lahiri, B. Mukhopadhyaya, Muon g-2 and a type-X two Higgs doublet scenario: some studies in high-scale validity. arXiv:2106.01449
100. V. Ilisie, New Barr-Zee contributions to $(g-2)_\mu$ in two-Higgs-doublet models. JHEP **04**, 077 (2015). https://doi.org/10.1007/JHEP04(2015)077 arXiv:1502.04199
101. T. Han, S.K. Kang, J. Sayre, Muon $g-2$ in the aligned two Higgs doublet model. JHEP **02**, 097 (2016). https://doi.org/10.1007/JHEP02(2016)097 arXiv:1511.05162
102. A. Cherchiglia, P. Kneschke, D. Stöckinger, H. Stöckinger-Kim, The muon magnetic moment in the 2HDM: complete two-loop result. JHEP **01**, 007 (2017). https://doi.org/10.1007/JHEP01(2017)007 arXiv:1607.06292
103. A. Cherchiglia, D. Stöckinger, H. Stöckinger-Kim, Muon g-2 in the 2HDM: maximum results and detailed phenomenology. Phys. Rev. D **98**, 035001 (2018). https://doi.org/10.1103/PhysRevD.98.035001 arXiv:1711.11567
104. S.-P. Li, X.-Q. Li, Y.-Y. Li, Y.-D. Yang, X. Zhang, Power-aligned 2HDM: a correlative perspective on $(g-2)_{e,\mu}$. JHEP **01**, 034 (2021). https://doi.org/10.1007/JHEP01(2021)034 arXiv:2010.02799
105. A. Crivellin, J. Heeck, P. Stoffer, A perturbed lepton-specific two-Higgs-doublet model facing experimental hints for physics beyond the Standard Model. Phys. Rev. Lett. **116**, 081801 (2016). https://doi.org/10.1103/PhysRevLett.116.081801 arXiv:1507.07567
106. Y. Omura, E. Senaha, K. Tobe, Lepton-flavor-violating Higgs decay $h \to \mu\tau$ and muon anomalous magnetic moment in a general two Higgs doublet model. JHEP **05**, 028 (2015). https://doi.org/10.1007/JHEP05(2015)028 arXiv:1502.07824
107. S. Iguro, Y. Omura, M. Takeuchi, Testing the 2HDM explanation of the muon g - 2 anomaly at the LHC. JHEP **11**, 130 (2019). https://doi.org/10.1007/JHEP11(2019)130 arXiv:1907.09845
108. S. Jana, V.P. K., S. Saad, Resolving electron and muon $g-2$ within the 2HDM. arXiv:2003.03386
109. W.-S. Hou, R. Jain, C. Kao, G. Kumar, T. Modak, Collider prospects for Muon $g-2$ in general two Higgs doublet model. arXiv:2105.11315
110. W.-S. Hou, G. Kumar, Charged lepton flavor violation in light of Muon $g-2$. arXiv:2107.14114
111. W.-S. Hou, Decadal mission for the new physics Higgs/flavor era. arXiv:2109.02557
112. O. Atkinson, M. Black, A. Lenz, A. Rusov, J. Wynne, Cornering the two Higgs doublet model type II. arXiv:2107.05650
113. D. Eriksson, J. Rathsman, O. Stal, 2HDMC: two-Higgs-doublet model calculator physics and manual. Comput. Phys. Commun. **181**, 189–205 (2010). https://doi.org/10.1016/j.cpc.2009.09.011 arXiv:0902.0851
114. M. Mühlleitner, M.O.P. Sampaio, R. Santos, J. Wittbrodt, ScannerS: parameter scans in extended scalar sectors. arXiv:2007.02985
115. M. Krause, M. Mühlleitner, M. Spira, 2HDECAY—a program for the calculation of electroweak one-loop corrections to Higgs decays in the Two-Higgs-Doublet Model including state-of-the-art QCD corrections. Comput. Phys. Commun. **246**, 106852 (2020). https://doi.org/10.1016/j.cpc.2019.08.003 arXiv:1810.00768
116. A. Denner, S. Dittmaier, A. Mück, PROPHECY4F 3.0: a Monte Carlo program for Higgs-boson decays into four-fermion final states in and beyond the Standard Model. Comput. Phys. Commun. **254**, 107336 (2020). https://doi.org/10.1016/j.cpc.2020.107336 arXiv:1912.02010
117. P. Bechtle, O. Brein, S. Heinemeyer, G. Weiglein, K.E. Williams, HiggsBounds: confronting arbitrary Higgs sectors with exclusion bounds from LEP and the tevatron. Comput. Phys. Commun. **181**, 138–167 (2010). https://doi.org/10.1016/j.cpc.2009.09.003 arXiv:0811.4169
118. P. Bechtle, O. Brein, S. Heinemeyer, G. Weiglein, K.E. Williams, HiggsBounds 2.0.0: confronting neutral and charged Higgs sector predictions with exclusion bounds from LEP and the tevatron. Comput. Phys. Commun. **182**, 2605–2631 (2011). https://doi.org/10.1016/j.cpc.2011.07.015 arXiv:1102.1898
119. P. Bechtle, O. Brein, S. Heinemeyer, O. Stal, T. Stefaniak, G. Weiglein et al., Recent developments in HiggsBounds and a preview of HiggsSignals. PoS **CHARGED2012**, 024 (2012). https://doi.org/10.22323/1.156.0024 arXiv:1301.2345
120. P. Bechtle, O. Brein, S. Heinemeyer, O. Stål, T. Stefaniak, G. Weiglein et al., $HiggsBounds-4$: improved tests of extended Higgs sectors against exclusion bounds from LEP, the tevatron and the LHC. Eur. Phys. J. C **74**, 2693 (2014). https://doi.org/10.1140/epjc/s10052-013-2693-2 arXiv:1311.0055
121. P. Bechtle, S. Heinemeyer, O. Stal, T. Stefaniak, G. Weiglein, Applying exclusion likelihoods from LHC searches to extended Higgs sectors. Eur. Phys. J. C **75**, 421 (2015). https://doi.org/10.1140/epjc/s10052-015-3650-z arXiv:1507.06706
122. O. Stål, T. Stefaniak, Constraining extended Higgs sectors with HiggsSignals. PoS **EPS–HEP2013**, 314 (2013). https://doi.org/10.22323/1.180.0314 arXiv:1310.4039
123. P. Bechtle, S. Heinemeyer, O. Stål, T. Stefaniak, G. Weiglein, $HiggsSignals$: confronting arbitrary Higgs sectors with measurements at the Tevatron and the LHC. Eur. Phys. J. C **74**, 2711 (2014). https://doi.org/10.1140/epjc/s10052-013-2711-4 arXiv:1305.1933
124. P. Bechtle, S. Heinemeyer, O. Stål, T. Stefaniak, G. Weiglein, Probing the Standard Model with Higgs signal rates from the Tevatron, the LHC and a future ILC. JHEP **11**, 039 (2014). https://doi.org/10.1007/JHEP11(2014)039 arXiv:1403.1582
125. F. Staub, From superpotential to model files for FeynArts and CalcHep/CompHep. Comput. Phys. Commun. **181**, 1077–1086 (2010). https://doi.org/10.1016/j.cpc.2010.01.011 arXiv:0909.2863
126. F. Staub, Automatic calculation of supersymmetric renormalization group equations and self energies. Comput. Phys. Commun. **182**, 808–833 (2011). https://doi.org/10.1016/j.cpc.2010.11.030 arXiv:1002.0840
127. F. Staub, SARAH 3.2: Dirac Gauginos, UFO output, and more. Comput. Phys. Commun. **184**, 1792–1809 (2013). https://doi.org/10.1016/j.cpc.2013.02.019 arXiv:1207.0906
128. F. Staub, SARAH 4: a tool for (not only SUSY) model builders. Comput. Phys. Commun. **185**, 1773–1790 (2014). https://doi.org/10.1016/j.cpc.2014.02.018 arXiv:1309.7223
129. W. Porod, SPheno, a program for calculating supersymmetric spectra, SUSY particle decays and SUSY particle production at e+ e- colliders. Comput. Phys. Commun. **153**, 275–315 (2003). https://doi.org/10.1016/S0010-4655(03)00222-4 arXiv:hep-ph/0301101
130. W. Porod, F. Staub, SPheno 3.1: extensions including flavour, CP-phases and models beyond the MSSM. Comput. Phys. Commun. **183**, 2458–2469 (2012). https://doi.org/10.1016/j.cpc.2012.05.021 arXiv:1104.1573
131. P. Athron, J.-H. Park, D. Stöckinger, A. Voigt, FlexibleSUSY—a spectrum generator generator for supersymmetric models. Com-

put. Phys. Commun. **190**, 139–172 (2015). https://doi.org/10.1016/j.cpc.2014.12.020 arXiv:1406.2319
132. P. Athron, J.-H. Park, T. Steudtner, D. Stöckinger, A. Voigt, Precise Higgs mass calculations in (non-)minimal supersymmetry at both high and low scales. JHEP **01**, 079 (2017). https://doi.org/10.1007/JHEP01(2017)079 arXiv:1609.00371
133. P. Athron, M. Bach, D. Harries, T. Kwasnitza, J.-H. Park, D. Stöckinger et al., FlexibleSUSY 2.0: extensions to investigate the phenomenology of SUSY and non-SUSY models. Comput. Phys. Commun. **230**, 145–217 (2018). https://doi.org/10.1016/j.cpc.2018.04.016 arXiv:1710.03760
134. P. Athron, A. Büchner, D. Harries, W. Kotlarski, D. Stöckinger, A. Voigt, FlexibleDecay: an automated calculator of scalar decay widths. arXiv:2106.05038
135. P. Athron, M. Bach, H.G. Fargnoli, C. Gnendiger, R. Greifenhagen, J.-H. Park et al., GM2Calc: precise MSSM prediction for $(g-2)$ of the muon. Eur. Phys. J. C **76**, 62 (2016). https://doi.org/10.1140/epjc/s10052-015-3870-2 arXiv:1510.08071
136. P.Z. Skands et al., SUSY Les Houches accord: interfacing SUSY spectrum calculators, decay packages, and event generators. JHEP **07**, 036 (2004). https://doi.org/10.1088/1126-6708/2004/07/036 arXiv:hep-ph/0311123
137. B.C. Allanach et al., SUSY Les Houches Accord 2. Comput. Phys. Commun. **180**, 8–25 (2009). https://doi.org/10.1016/j.cpc.2008.08.004 arXiv:0801.0045
138. GAMBIT collaboration, P. Athron et al., GAMBIT: the global and modular beyond-the-standard-model inference tool. Eur. Phys. J. C **77**, 784 (2017). https://doi.org/10.1140/epjc/s10052-017-5321-8. arXiv:1705.07908
139. GAMBIT Models Workgroup collaboration, P. Athron et al., SpecBit, DecayBit and PrecisionBit: GAMBIT modules for computing mass spectra, particle decay rates and precision observables. Eur. Phys. J. C **78**, 22 (2018). https://doi.org/10.1140/epjc/s10052-017-5390-8. arXiv:1705.07936
140. S.M. Barr, A. Zee, Electric dipole moment of the electron and of the neutron. Phys. Rev. Lett. **65**, 21–24 (1990). https://doi.org/10.1103/PhysRevLett.65.21
141. D. Chang, W.-F. Chang, C.-H. Chou, W.-Y. Keung, Large two loop contributions to g-2 from a generic pseudoscalar boson. Phys. Rev. D **63**, 091301 (2001). https://doi.org/10.1103/PhysRevD.63.091301 arXiv:hep-ph/0009292
142. K.-M. Cheung, C.-H. Chou, O.C.W. Kong, Muon anomalous magnetic moment, two Higgs doublet model, and supersymmetry. Phys. Rev. D **64**, 111301 (2001). https://doi.org/10.1103/PhysRevD.64.111301 arXiv:hep-ph/0103183
143. Y.-L. Wu, Y.-F. Zhou, Muon anomalous magnetic moment in the standard model with two Higgs doublets. Phys. Rev. D **64**, 115018 (2001). https://doi.org/10.1103/PhysRevD.64.115018 arXiv:hep-ph/0104056
144. M. Krawczyk, Precision muon g-2 results and light Higgs bosons in the 2HDM(II). Acta Phys. Polon. B **33**, 2621–2634 (2002). arXiv:hep-ph/0208076
145. A. Davydychev, J. Tausk, Two-loop self-energy diagrams with different masses and the momentum expansion. Nucl. Phys. B **397**, 123–142 (1993). https://doi.org/10.1016/0550-3213(93)90338-P
146. J.F. Gunion, H.E. Haber, The CP conserving two Higgs doublet model: the approach to the decoupling limit. Phys. Rev. D **67**, 075019 (2003). https://doi.org/10.1103/PhysRevD.67.075019 arXiv:hep-ph/0207010
147. D. Lopez-Val, J. Sola, Delta r in the two-Higgs-doublet model at full one loop level- and beyond. Eur. Phys. J. C **73**, 2393 (2013). https://doi.org/10.1140/epjc/s10052-013-2393-y arXiv:1211.0311
148. G. Degrassi, G.F. Giudice, QED logarithms in the electroweak corrections to the muon anomalous magnetic moment. Phys. Rev. D **58**, 053007 (1998). https://doi.org/10.1103/PhysRevD.58.053007 arXiv:hep-ph/9803384
149. G. Guennebaud, B. Jacob et al., Eigen v3 (2010). http://eigen.tuxfamily.org
150. Boost, Boost C++ Libraries (2021). http://www.boost.org/
151. W. R. Inc., Mathematica
152. G. van Rossum, Python. http://www.python.org
153. W.T. Lavrijsen, A. Dutta, High-performance Python–C++ bindings with PyPy and Cling (2018). http://cern.ch/wlav/Cppyy_LavrijsenDutta_PyHPC16.pdf
154. Particle Data Group collaboration, P. Zyla et al., Review of particle physics. PTEP **2020**, 083C01 (2020). https://doi.org/10.1093/ptep/ptaa104